Supplementary Information

Tunable cyclic operation of dissipative molecular switches based on anion recognition

Xin Zhang,*† Lijun Mao,† Rongjing He, Yanting Shi, Lingyi Li, Shuo Li, Chenghao Zhu, Yanjing Zhang, Da Ma*

School of Pharmaceutical Engineering & Institute for Advanced Studies, Taizhou University, 1139 Shifu Avenue, Taizhou 318000, Zhejiang, China

†Equal contribution

Email: zx91318@163.com; dama@tzc.edu.cn

Contents

1. General information

4,4'-Biphenyldicarboxylic acid (**2**) or 2,6'-naphthalenedicarboxylic acid (**3**) were purchased commercially (Bide Pharmatech) and used without further purification. 2,1,3-Benzothiadiazole, 1,3,5-trioxane, hydrobromic acid (48 wt. % in H_2O), 2,6-dibromopyridine, imidazole, copper(I) iodide, K_2CO_3, L-proline, trichloroacetic acid and ammonium hexafluorophosphate were purchased from Energy Chemistry (Shanghai). Deuterated solvents were purchased from Cambridge Isotope Laboratory (Andover, MA). All solvents were dried according to the standard procedures and all of them were degassed under N_2 for 30 minutes before use. All air-sensitive reactions were carried out under inert N_2 atmosphere.

^{1}H and ^{13}C NMR spectra were recorded at 400 MHz with a Mercury plus 400 spectrometer at 298 K. The ^{1}H and ^{13}C NMR chemical shifts are reported relative to the residual solvent signals. Coupling constants (*J*) are denoted in Hz and chemical shifts (δ) in ppm. Multiplicities are denoted as follows: s = singlet, d = doublet. 2D NMR spectra (NOESY) were recorded on Bruker 400 MHz Spectrometer at 298 K. UV-vis spectra were measured by SHIMADZU UV-2450. Fluorescence emission spectra were collected on a SHIMADZU RF6000 spectrometer.

2. Synthesis and characterization of [1^{4+}•$4PF_6^-$]

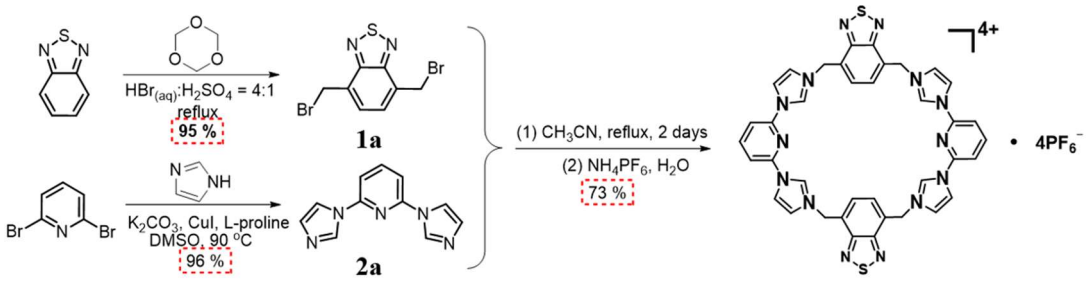

Scheme S1. The synthesis route to [$\mathbf{1}^{4+}$•$4PF_6^-$].

*Synthesis of compound **1a***

Following a modified literature procedure[S1-S2]: A three-necked roundbottom flask equipped with a magnetic stir bar and condenser was added 2,1,3-benzothiadiazole (5.00 g, 36.7 mmol), hydrobromic acid (48 wt% in water, 100 mL) and sulfuric acid (conc., 25 mL). 1,3,5-trioxane (16.5 g, 184 mmol) and myristyltrimethylammonium bromide (1.23 g, 3.67 mmol) were added to the flask while stirring the mixture. The reaction was heated to reflux and stirred for 24 hours. The reaction was cooled to room temperature and the precipitate was filtered, washed with water then ethanol and dried under reduced pressure to afford compound **1a** as a white solid (11.2 g, 95%). ^{1}H NMR (400 MHz, Chloroform-*d*) δ 7.63 (s, 2H), 4.97 (s, 4H).

*Synthesis of compound **2a***

Following a modified literature procedure[S3]: A three-necked roundbottom flask was charged with 2,6-dibromopyridine (6.00 g, 25.3 mmol), imidazole (3.70 g, 54.3 mmol), K_2CO_3 (10.5 g, 75.9 mmol), CuI (762 mg, 4.00 mmol), and L-proline (921 mg, 8.00 mmol). It was then evacuated and backfilled with nitrogen three times. DMSO (30 mL) was then added to the flask by syringe at room temperature under nitrogen, and the mixture was then heated at 363 K. After 48 h, the reaction was cooled and partitioned between 250 mL of water and 250 mL of dichloromethane. The organic layer was isolated, and the aqueous layer was extracted three times with dichloromethane (total 250 mL). The combined organic layers were washed with water ten times, and dried over Na_2SO_4. The solvent was removed using a rotary evaporation and the residual solid was recrystallized from a mixture of dichloromethane and hexane to afford compound **2a** as a grey solid (5.10 g, yield: 96%). The characterization data for this product matches that found in the literature. [S4]

Synthesis of compound [$\mathbf{1}^{4+}$•$4PF_6^-$]

A solution of **1a** (322 mg, 1.00 mmol) in acetonitrile (150 mL) was added dropwise to a solution of **2a** (211 mg, 1.00 mmol) in acetonitrile (150 mL) over a period of 12 h. The mixture was heated under reflux for 48 h. After cooling to room temperature, the solvent was removed via rotary evaporation. The residue was dissolved in water (300 mL) and NH_4PF_6 (1.63 g, 10.0 mmol) was added to the solution. This gave rise to a

white precipitate, which was filtered off and washed with 500 mL water. The crude product was recrystallized from acetonitrile to afford compound $\mathbf{1}^{4+}\cdot 4PF_6^-$ white solid (450 mg, 73%). ^{1}H NMR (400 MHz, DMSO-d_6) δ 10.31 (br, 4H), 8.65 (dd, J = 3.6, 1.6 Hz, 4H), 8.62 (t, J = 8.4 Hz, 2H), 8.24 (d, J = 8.0 Hz, 4H), 8.21 (dd, J = 3.6, 1.6 Hz, 4H), 7.69 (s, 8H), 6.06 (s, 8H). ^{13}C NMR (100 MHz, DMSO-d_6) δ 153.1, 145.6, 145.5, 136.7, 129.3, 128.4, 125.4, 120.3, 115.4, 50.1. HR-MS (ESI) m/z calculated for $C_{38}H_{30}N_{14}F_{18}P_3S_2$ [$\mathbf{1}^{4+}\cdot 3PF_6^-$] 1181.1150, found: 1181.1152.

3. Synthesis of chemical fuels

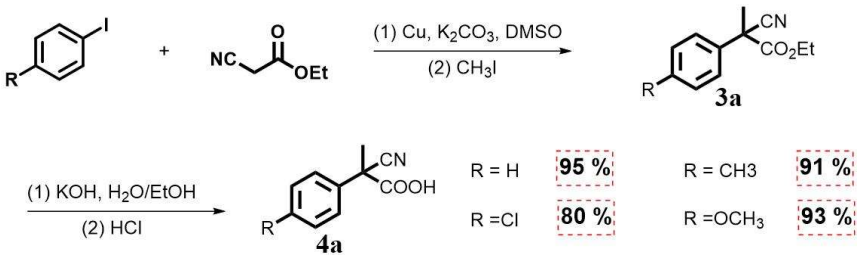

Scheme S2. The synthesis route to chemical fuels

*Synthesis of compound **3a***

Following a modified literature procedure[S5]: Iodobenzene (5.00 g, 24.5 mmol) and Ethyl cyanoacetate (5.50 g, 49.0 mmol) were added sequentially to a suspension of K_2CO_3 (13.5 g, 97.7 mmol) in DMSO (50 mL), resulting in a white suspension. A solution of CuI (466 mg, 2.45 mmol) in DMSO (1 mL) was then added. The resulting mixture was heated at 60°C for 24 h. The reaction was cooled to room temperature. Then, the resulting mixture was treated with iodomethane (3.05 mL) at room temperature for 4 h after which it was poured into water, extracted with ether. The organic layer was dried over sodium sulfate, concentrated, and chromatographed (SiO_2, CH_2Cl_2) to give **3a** as a white oil (4.50 g, 90%). The characterization data for this product matches that found in the literature.[S6-S8]

*Synthesis of compound **4a***

Following a modified literature procedure[S9]: ethyl 2-cyano-2-phenylpropanoate (4.50 g, 22.2 mmol) was suspended in a solution of KOH (6.20 g, 111 mmol) in water (50 mL) and EtOH (20 mL). After the mixture was stirred for 24 h, the alcohol was removed in vacuo at room temp. Water was added to fully dissolve the potassium salt and the solution was saturated with NaCl. The water phase was extracted four times with dichloromethane (dichloromethane extracts discarded) and was then acidified with HCl at 0°C. The product was isolated by being extracted with dichloromethane three times. After the solvent was removed at room temp, the resulting solid was dissolved in hexanes/ethyl acetate. Cooling to -40 °C afforded **4a** (3.70 g, 95%) as colorless solid. The characterization data for this product matches that found in the literature.[S10]

4. Host-guest complexation

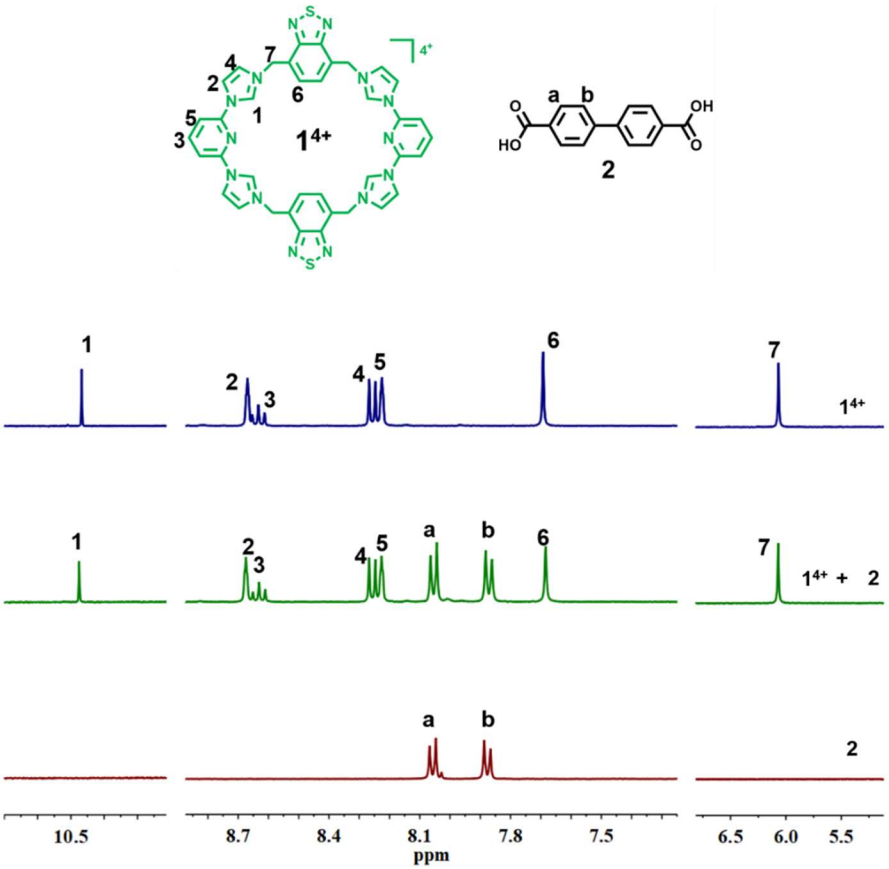

Fig. S1 Partial ^{1}H NMR (400 MHz, 298 K) spectra of 1.00 mM $\mathbf{1}^{4+}$ (top), a mixture of 1.00 mM $\mathbf{1}^{4+}$ and 1.00 mM **2** (middle) and 1.00 mM **2** (bottom) in DMSO-d_6.

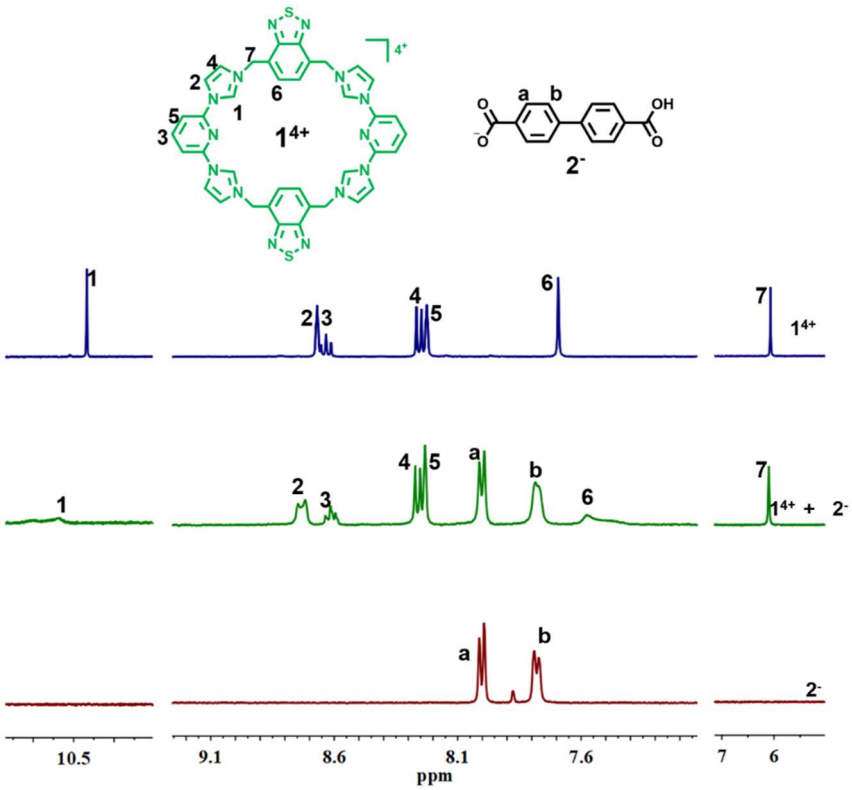

Fig. S2 Partial ^{1}H NMR (400 MHz, 298 K) spectra of 1.00 mM $\mathbf{1}^{4+}$ (top), a mixture of 1.00 mM $\mathbf{1}^{4+}$ and 1.00 mM $\mathbf{2}^{-}$ (middle) and 1.00 mM $\mathbf{2}^{-}$ (bottom) in DMSO-d_6.

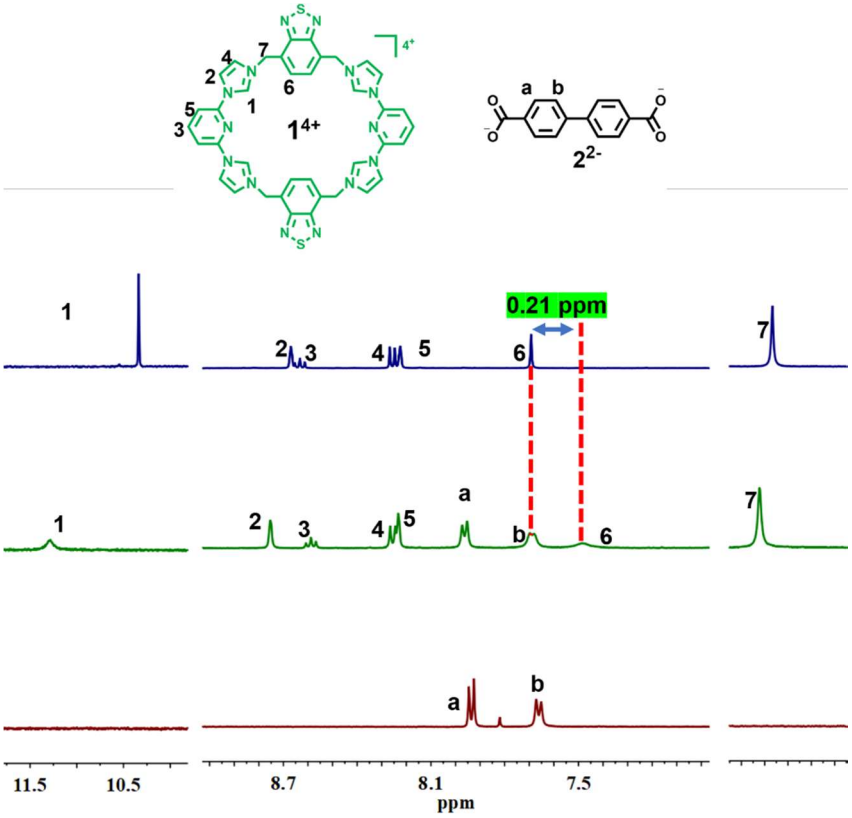

Fig. S3 Partial ^{1}H NMR (400 MHz, 298 K) spectra of 1.00 mM $\mathbf{1}^{4+}$ (top), a mixture of 1.00 mM $\mathbf{1}^{4+}$ and 1.00 mM $\mathbf{2}^{2-}$ (middle) and 1.00mM $\mathbf{2}^{2-}$ (bottom) in DMSO-d_6.

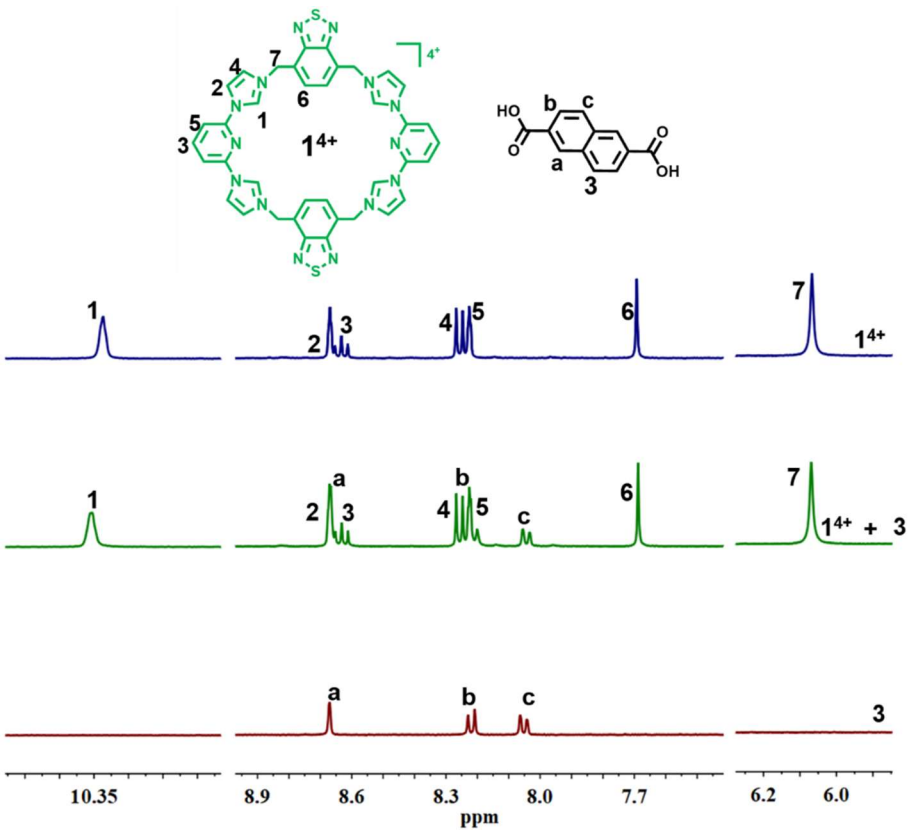

Fig. S4 Partial ^{1}H NMR (400 MHz, 298 K) spectra of 1.00 mM $\mathbf{1}^{4+}$ (top), a mixture of 1.00 mM $\mathbf{1}^{4+}$ and 1.00 mM **3** (middle) and 1.00 mM **3** (bottom) in DMSO-d_6.

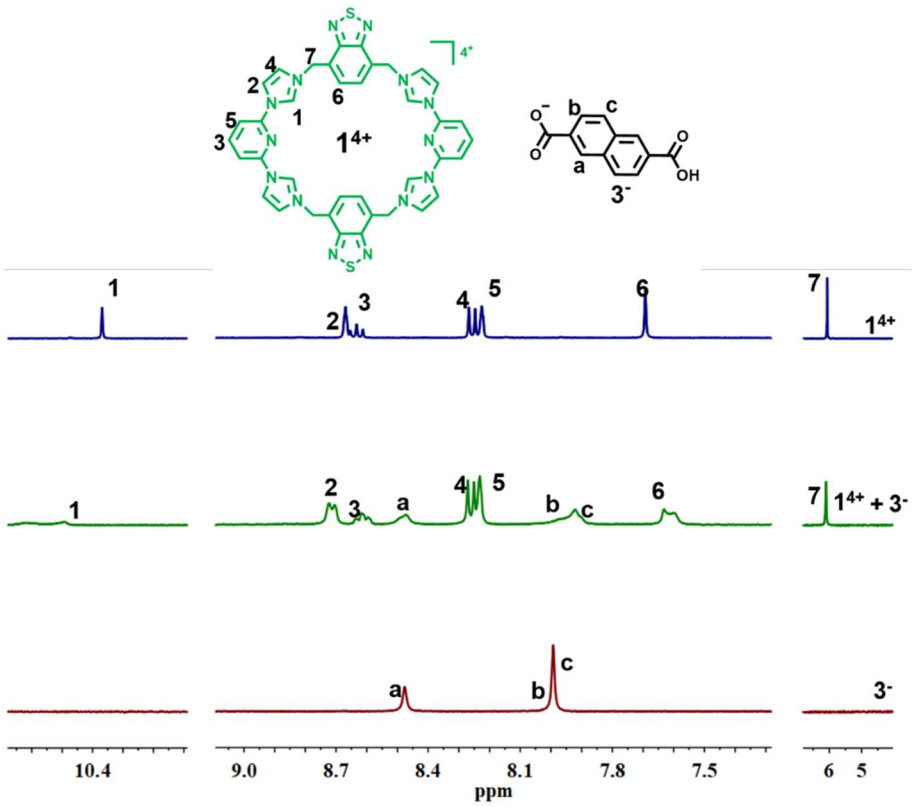

Fig. S5 Partial ^{1}H NMR (400 MHz, 298 K) spectra of 1.00 mM $\mathbf{1}^{4+}$ (top), a mixture of 1.00 mM $\mathbf{1}^{4+}$ and 1.00 mM $\mathbf{3}^{-}$ (middle) and 1.00 mM $\mathbf{3}^{-}$ (bottom) in DMSO-d_6.

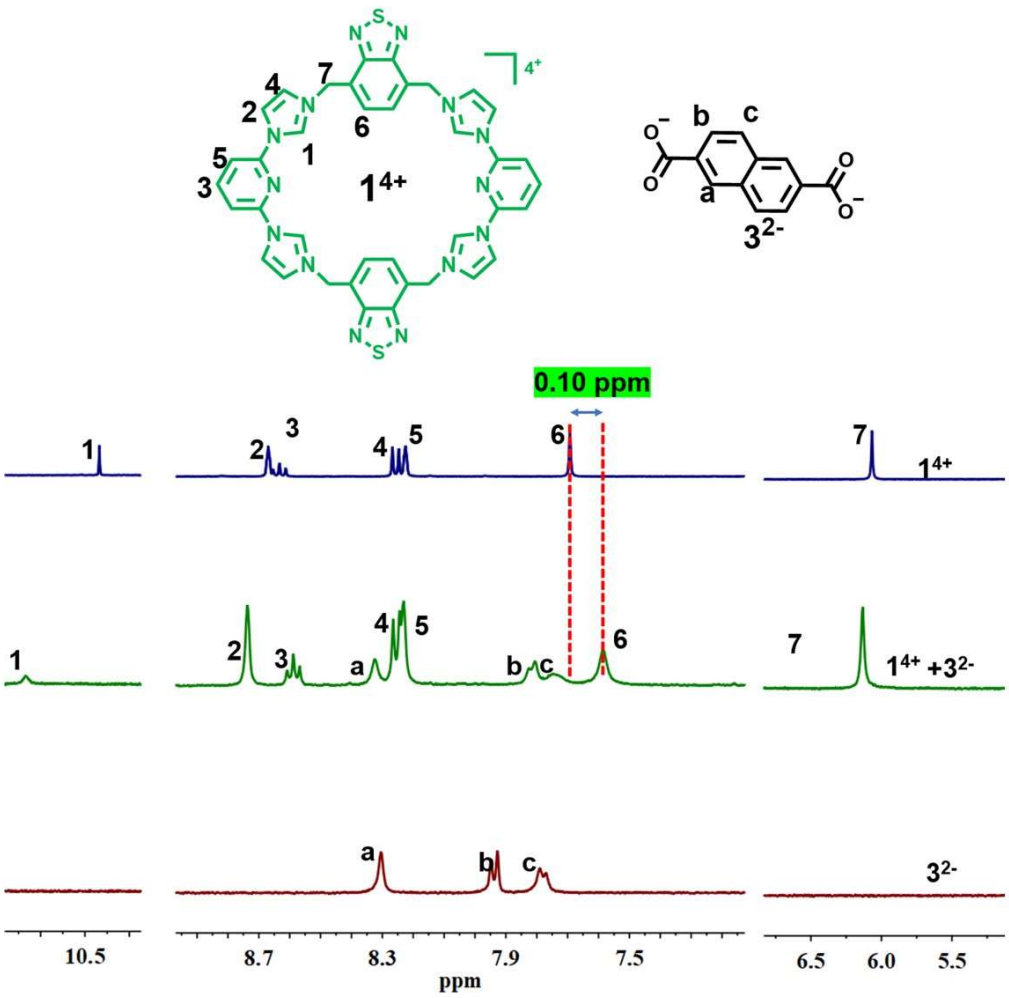

Fig. S6 Partial ^{1}H NMR (400 MHz, 298 K) spectra of 1.00 mM $\mathbf{1}^{4+}$ (top), a mixture of 1.00 mM $\mathbf{1}^{4+}$ and 1.00 mM $\mathbf{3}^{2-}$ (middle) and 1.00 mM $\mathbf{3}^{2-}$ (bottom) in DMSO-d_6.

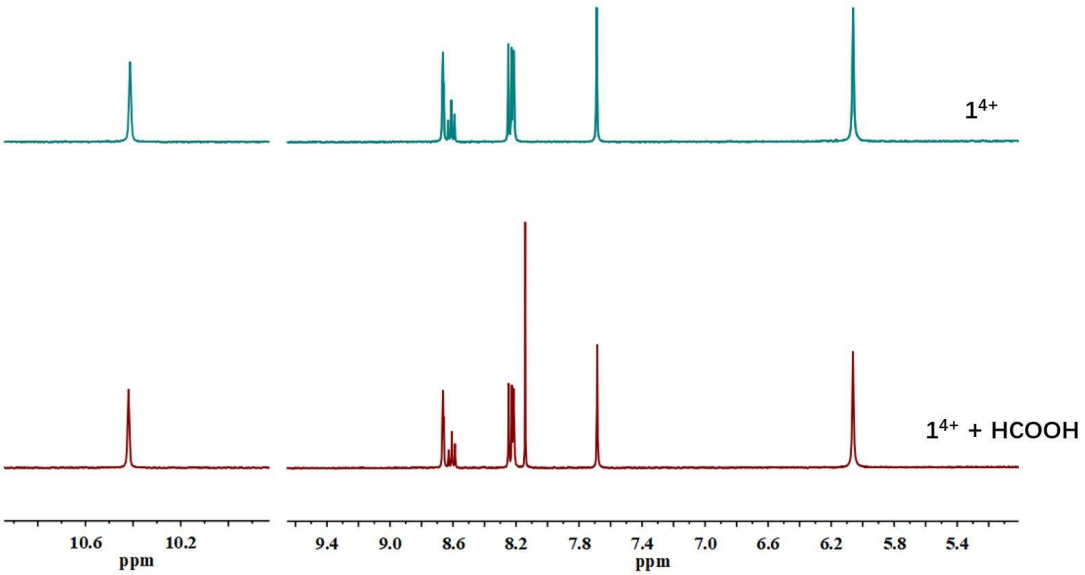

Fig. S7 Partial ^{1}H NMR (400 MHz, 298 K) spectra of 1.00 mM $\mathbf{1}^{4+}$ (top) and a mixture of 1.00 mM $\mathbf{1}^{4+}$ with 2.00 equiv HCOOH (bottom) in DMSO-*d*6.

5. Solution study of the complexation

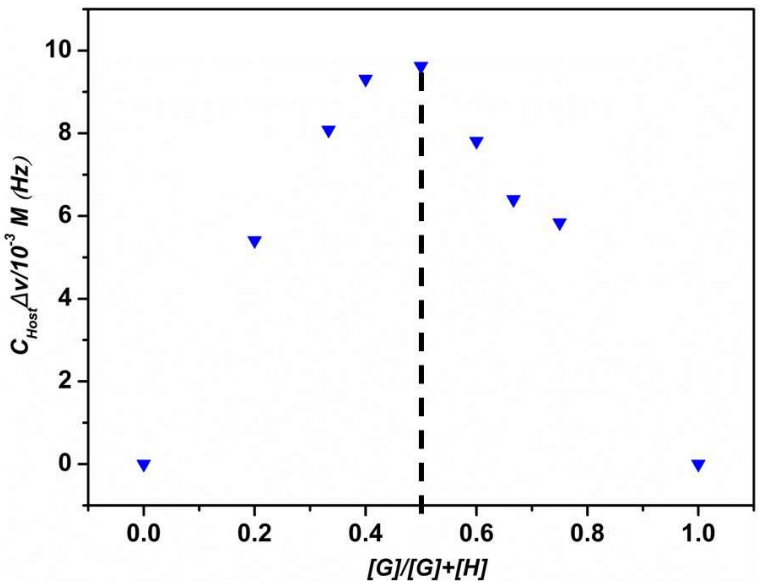

Fig. S8 ^{1}H NMR spectral Job plot corresponding to the interaction between $\mathbf{1}^{4+}$•$4PF_6^-$ and $\mathbf{2}^-$) ([host] + [guest] = 1.00 mM). Maximum value was 0.5, a finding consistent with (but not a proof of) a 1:1 (host: guest) binding stoichiometry.

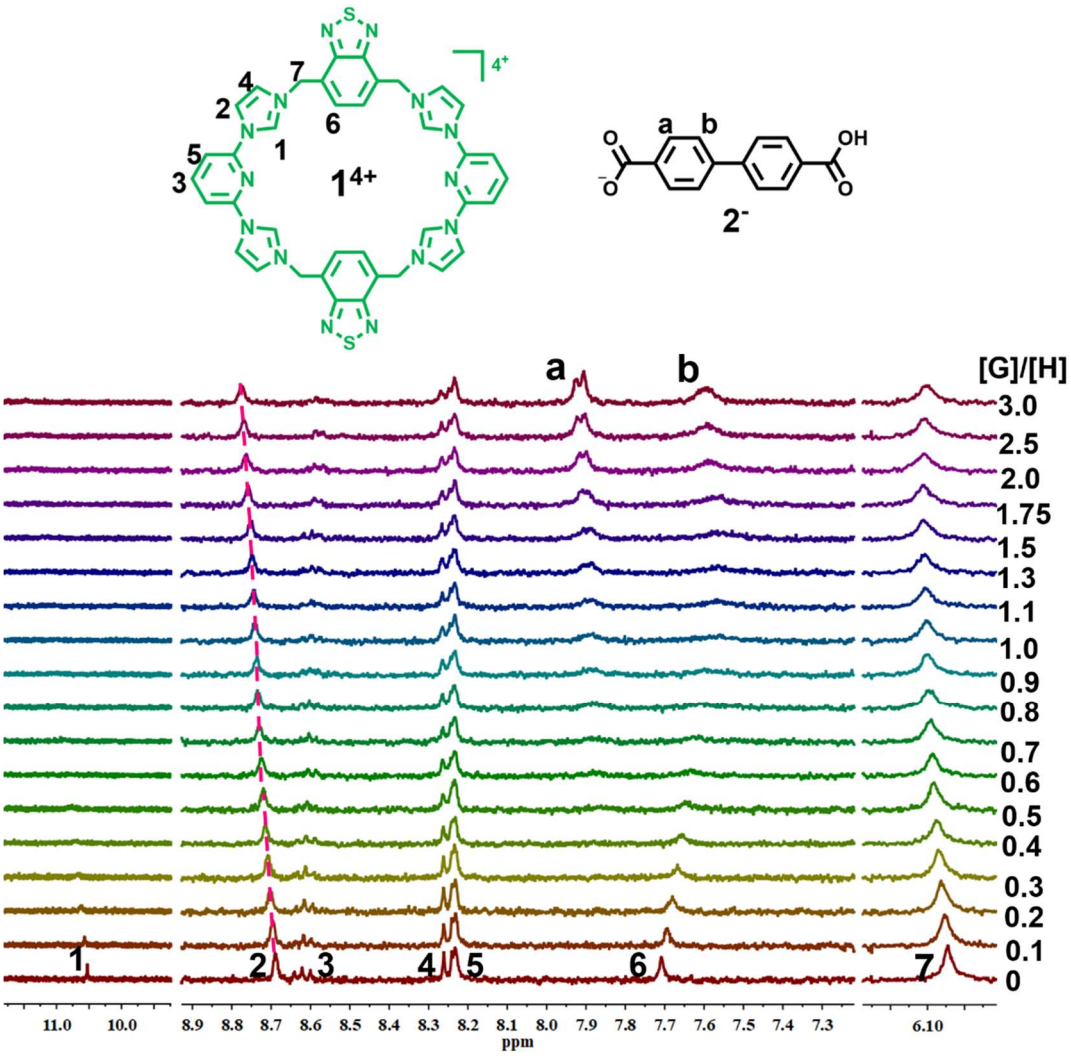

Fig. S9. 400 MHz ^{1}H NMR spectroscopic titration of $\mathbf{1}^{4+}$•4PF_6^- (maintained at 0.1 mM) with increasing 4,4'-biphenyldicarboxylate monoanion ($\mathbf{2}^-$) in DMSO-d_6 at 298 K.

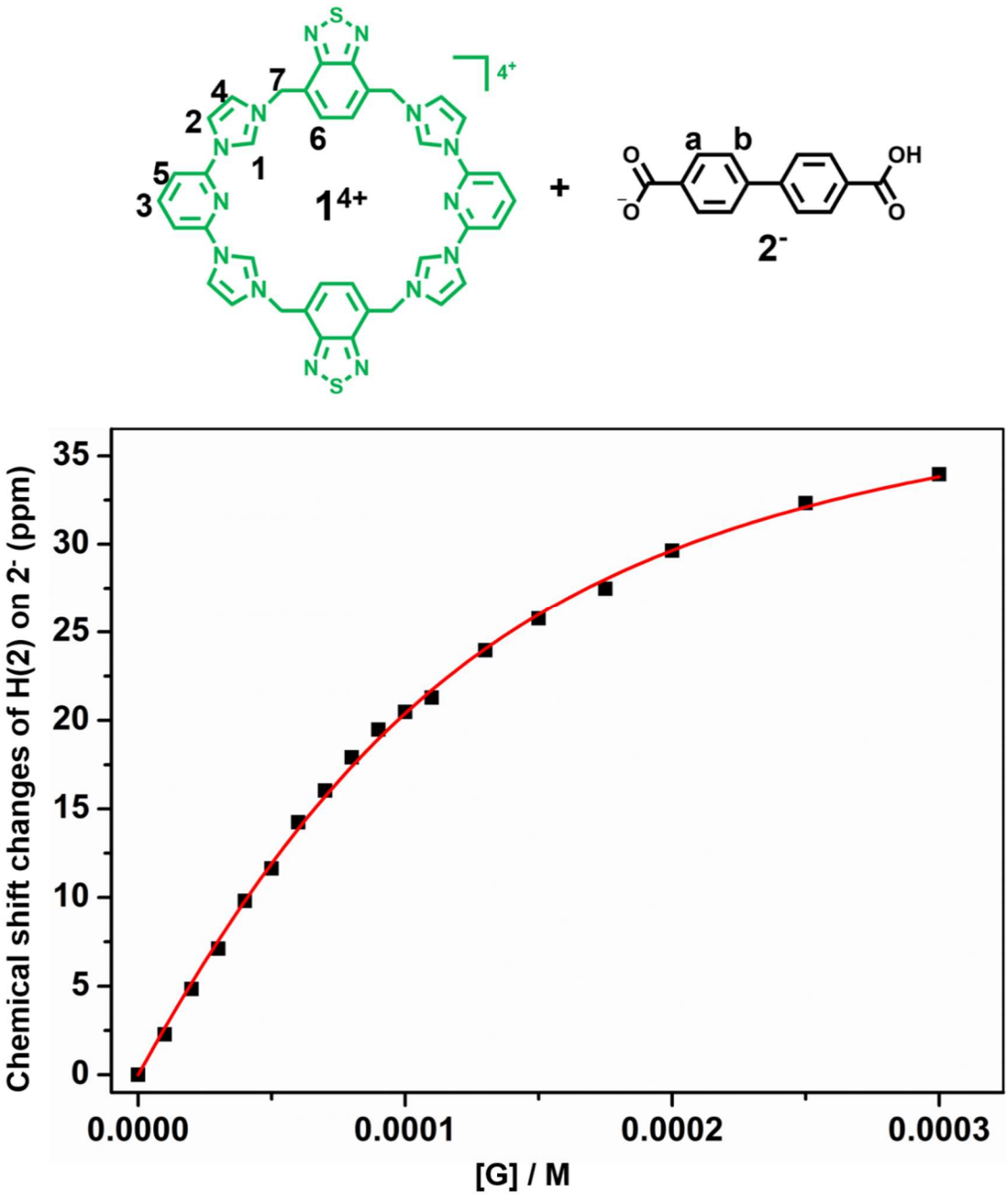

Fig. S10. ^{1}H NMR spectral binding isotherms corresponding to the interaction between $\mathbf{1}^{4+}$•4PF$_6^-$ and 4,4'-biphenyldicarboxylate monoanion ($\mathbf{2}^-$) in DMSO-d_6 at 298 K. The chemical shift changes of H (2) on $\mathbf{1}^{4+}$ were used for the calculation of $K_a = (1.7 \pm 0.1) \times 10^4\ M^{-1}$, corresponding to the formation of the initial 1:1 complex $[\mathbf{1}^{4+}\bullet\mathbf{2}^-]^{3+}$, Fitting result based on proton 2 of $\mathbf{2}^-$.

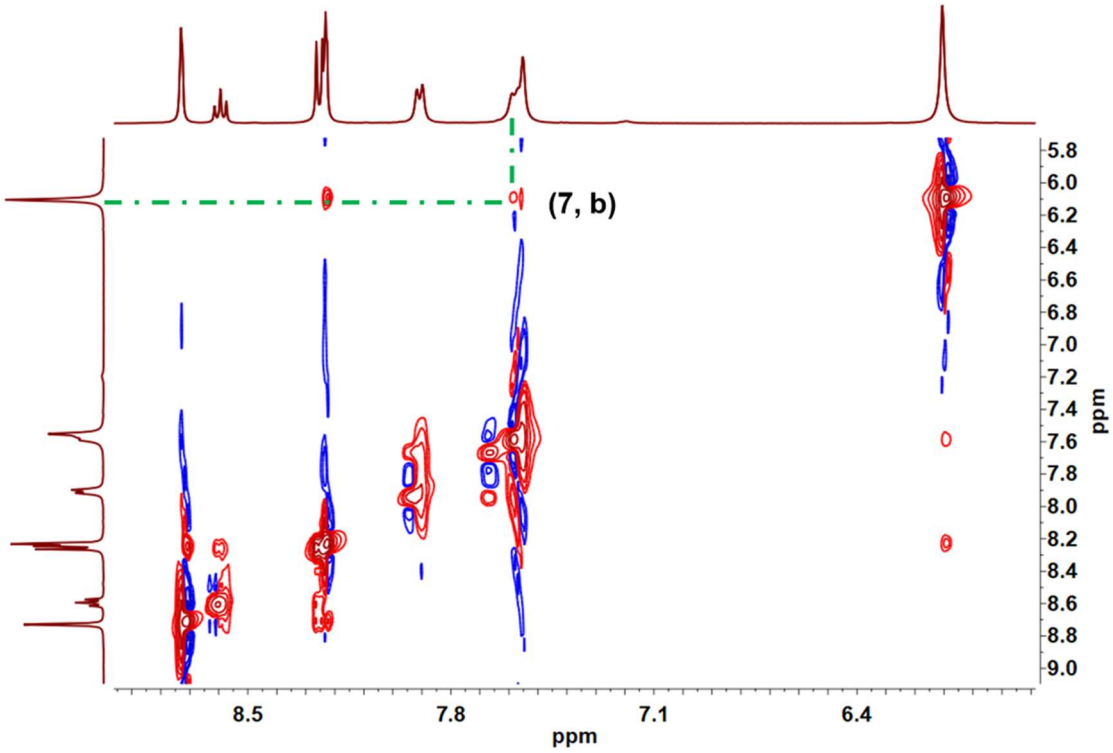

Fig. S11 NOESY spectrum of $\mathbf{1}^{4+}$•4PF_6^- (10.0 mM) recorded in the presence of 1 molar equiv of $\mathbf{2}^-$ in DMSO-d_6 at 298 K. Through-space NOE was observed between H_7 on host $\mathbf{1}^{4+}$ and H_b on guest $\mathbf{2}^-$, which is taken as evidence that the host-guest interactions between macrocycle $\mathbf{1}^{4+}$ and guest anionic species $\mathbf{2}^-$.

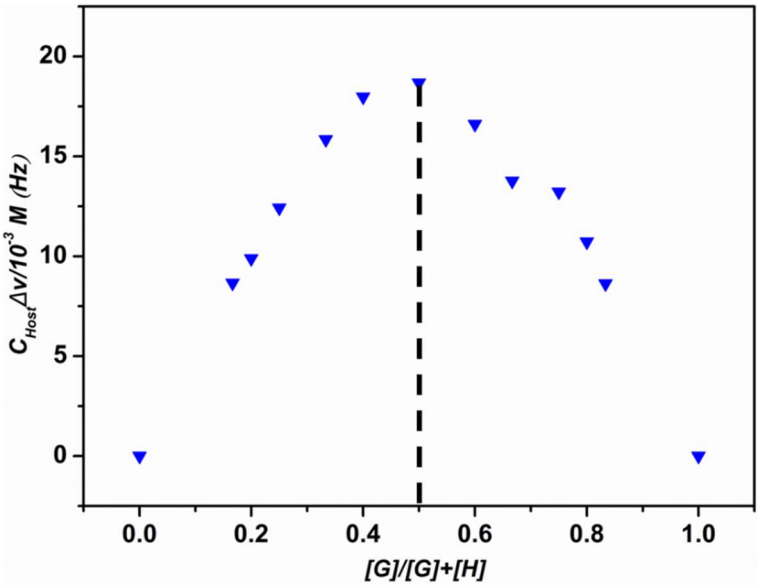

Fig. S12 ^{1}H NMR spectral Job plot corresponding to the interaction between $\mathbf{1}^{4+}$•4PF_6^- and $\mathbf{2}^{2-}$ ([host] + [guest] = 1.00 mM). Maximum value was 0.5, a finding consistent with (but not a proof of) a 1:1 (host: guest) binding stoichiometry.

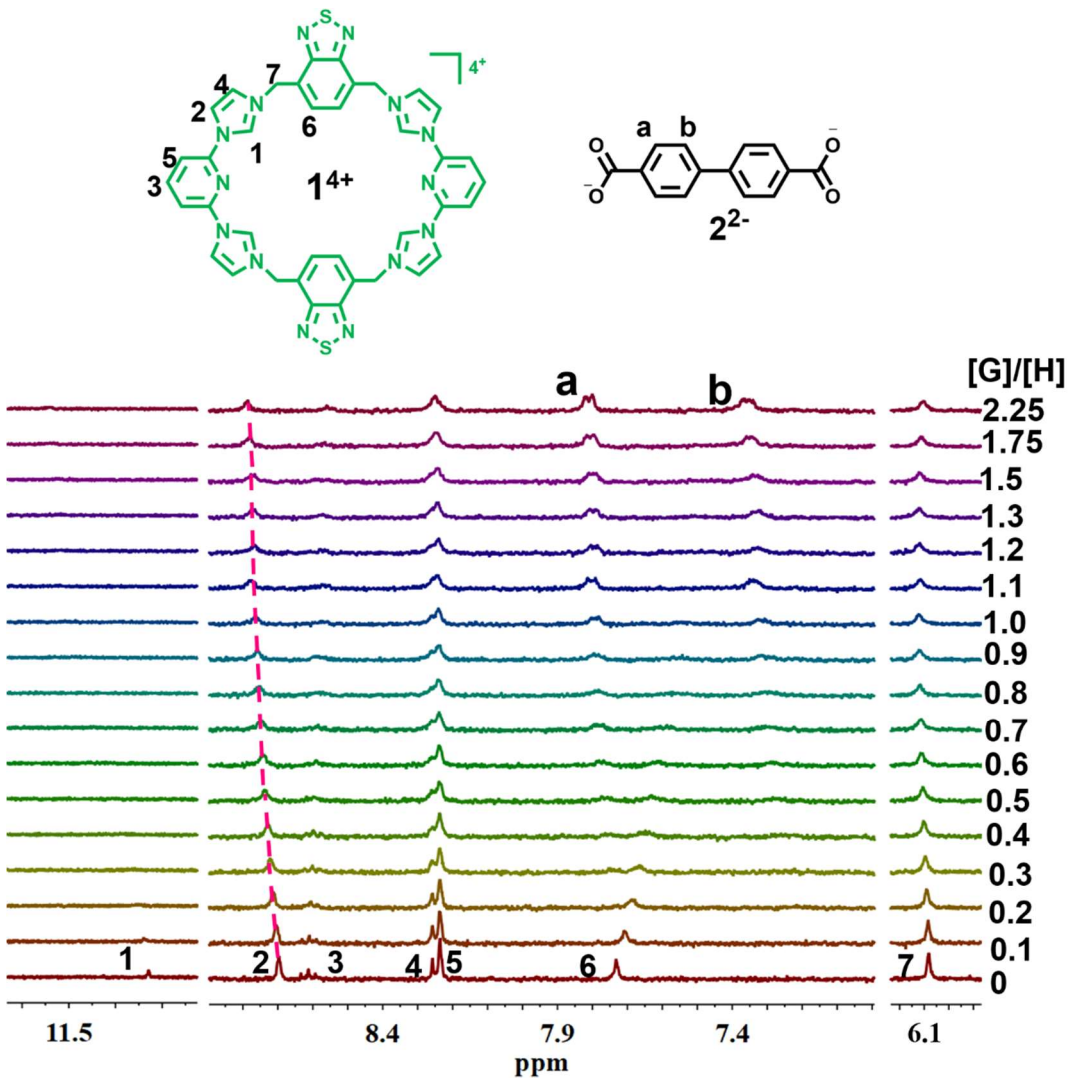

Fig. S13 400 MHz ^{1}H NMR spectroscopic titration of $\mathbf{1}^{4+}$•4PF_6^- (maintained at 0.1 mM) with increasing 4,4'-biphenyldicarboxylate dianion ($\mathbf{2}^{2-}$) in DMSO-d_6 at 298 K.

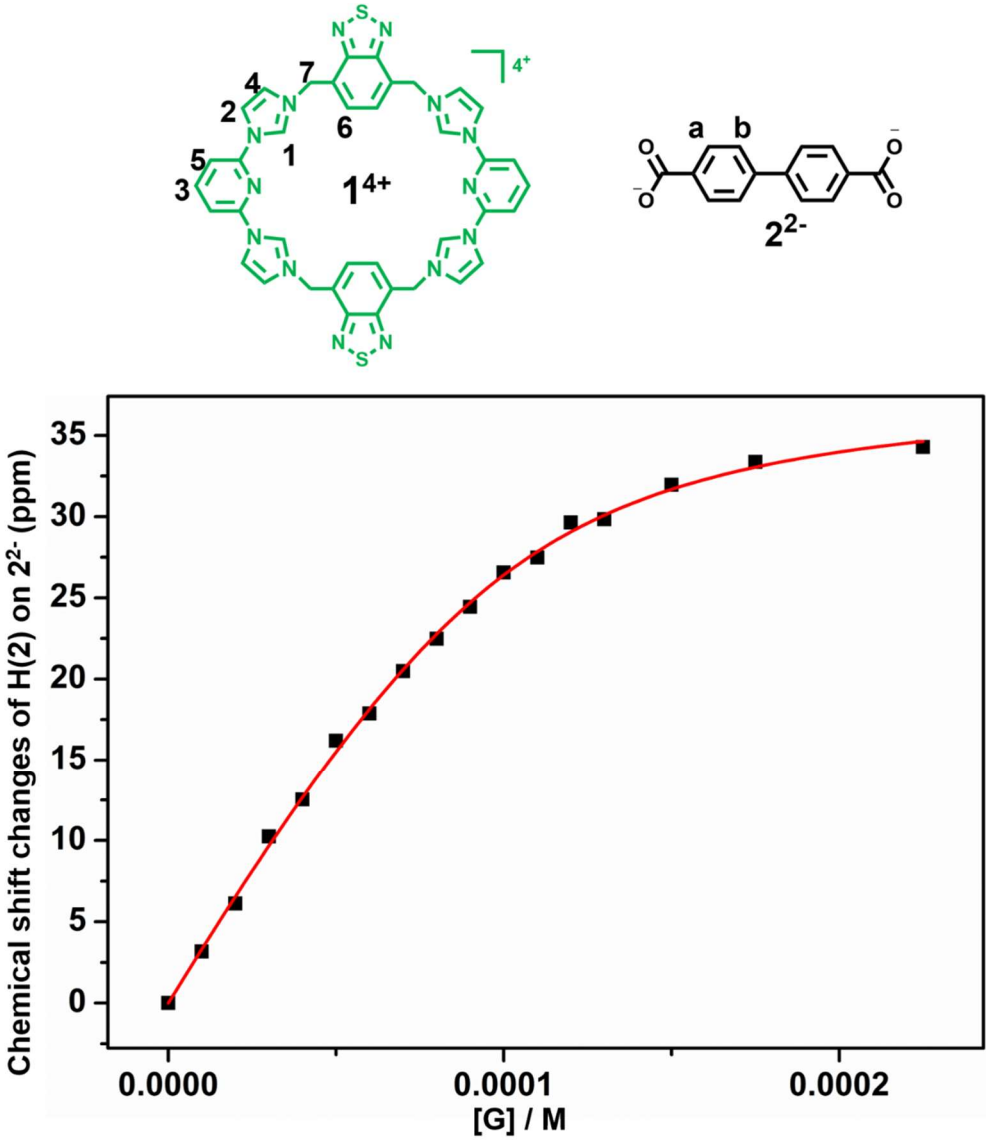

Fig. S14 ^{1}H NMR spectral binding isotherms corresponding to the interaction between $\mathbf{1}^{4+}$•4PF_6^- and 4,4'-biphenyldicarboxylate dianion ($\mathbf{2}^{2-}$) in DMSO-d_6 at 298 K. The chemical shift changes of H (1) on $\mathbf{1}^{4+}$ were used for the calculation of K_a = (7.2 ± 0.8) × 10^4 M^{-1}, corresponding to the formation of the initial 1:1 complex [$\mathbf{1}^{4+}$•$\mathbf{2}^-$]$^{3+}$, Fitting result based on proton 2 of $\mathbf{2}^{2-}$.

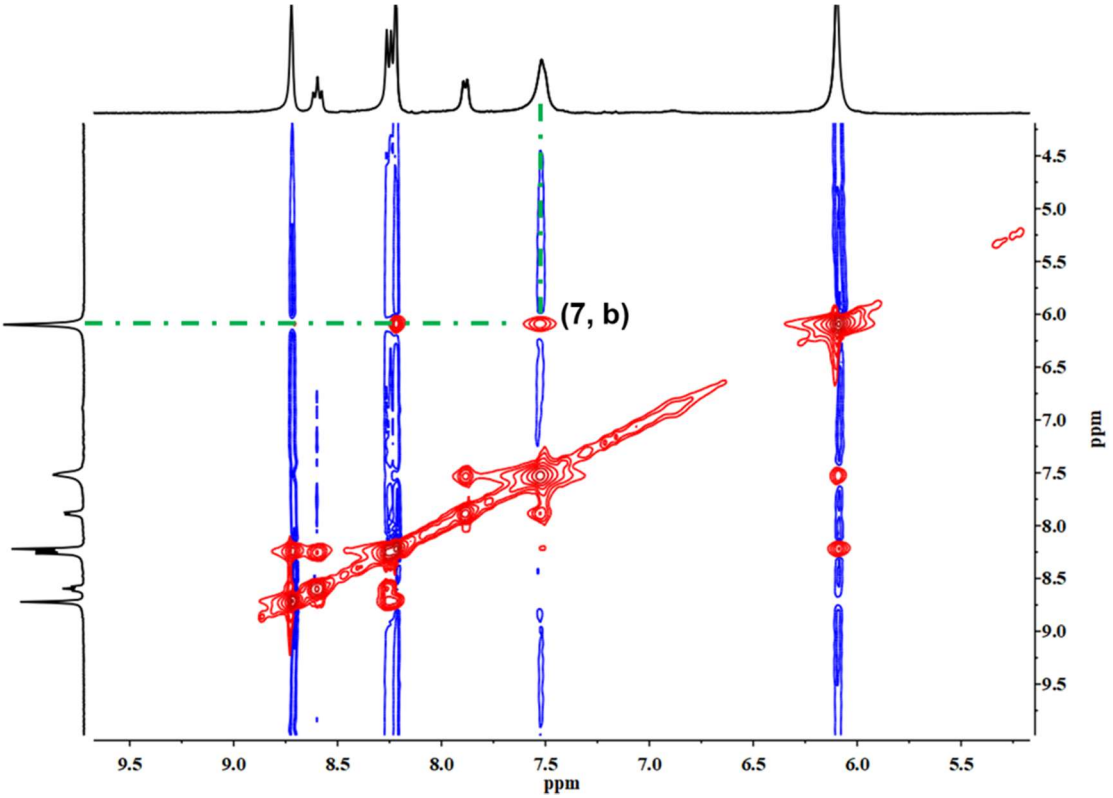

Fig. S15 NOESY spectrum of $\mathbf{1}^{4+}$•$4PF_6^-$ (10.0 mM) recorded in the presence of 1 molar equiv of $\mathbf{2}^{2-}$ in DMSO-d_6 at 298 K. Through-space NOE was observed between H_7 on host $\mathbf{1}^{4+}$ and H_b on guest $\mathbf{2}^-$, which is taken as evidence that the host-guest interactions between macrocycle $\mathbf{1}^{4+}$ and guest anionic species $\mathbf{2}^{2-}$.

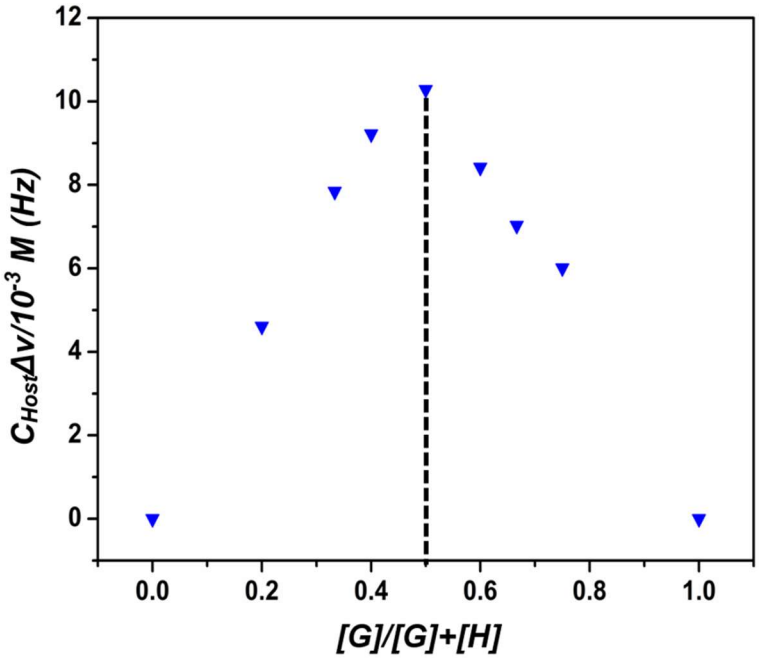

Fig. S16 ^{1}H NMR spectral Job plot corresponding to the interaction between $\mathbf{1}^{4+}$•$4PF_6^-$ and $\mathbf{3}^-$ ([host] + [guest] = 1.00 mM). Maximum value was 0.5, a finding consistent with (but not a proof of) a 1:1 (host: guest) binding stoichiometry.

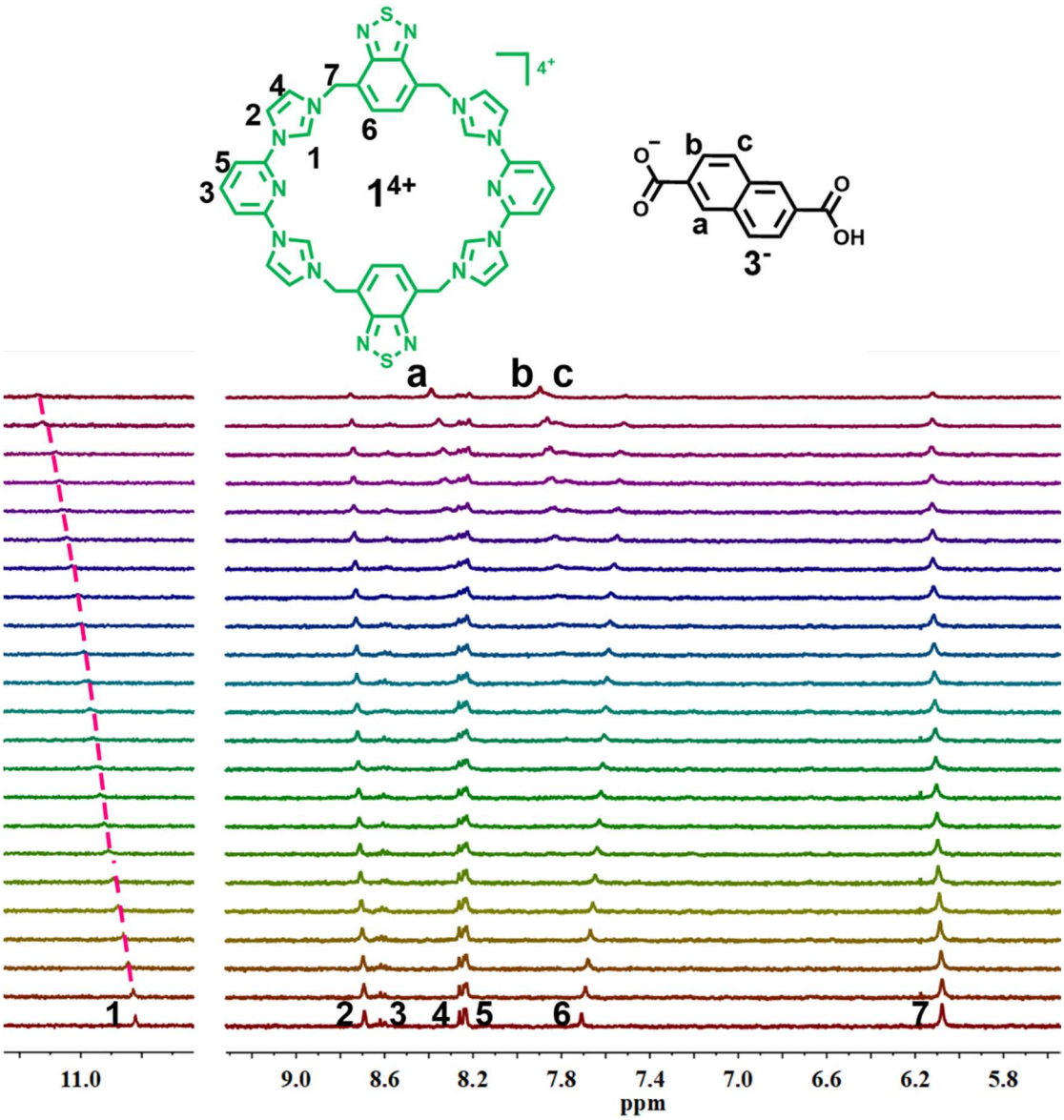

Fig. S17 400 MHz ^{1}H NMR spectroscopic titration of $\mathbf{1}^{4+}$•4PF_6^- (maintained at 0.5 mM) with increasing 2,6'-naphthalenedicarboxylate monoanion (**3**$^-$) in DMSO-d_6 at 298 K.

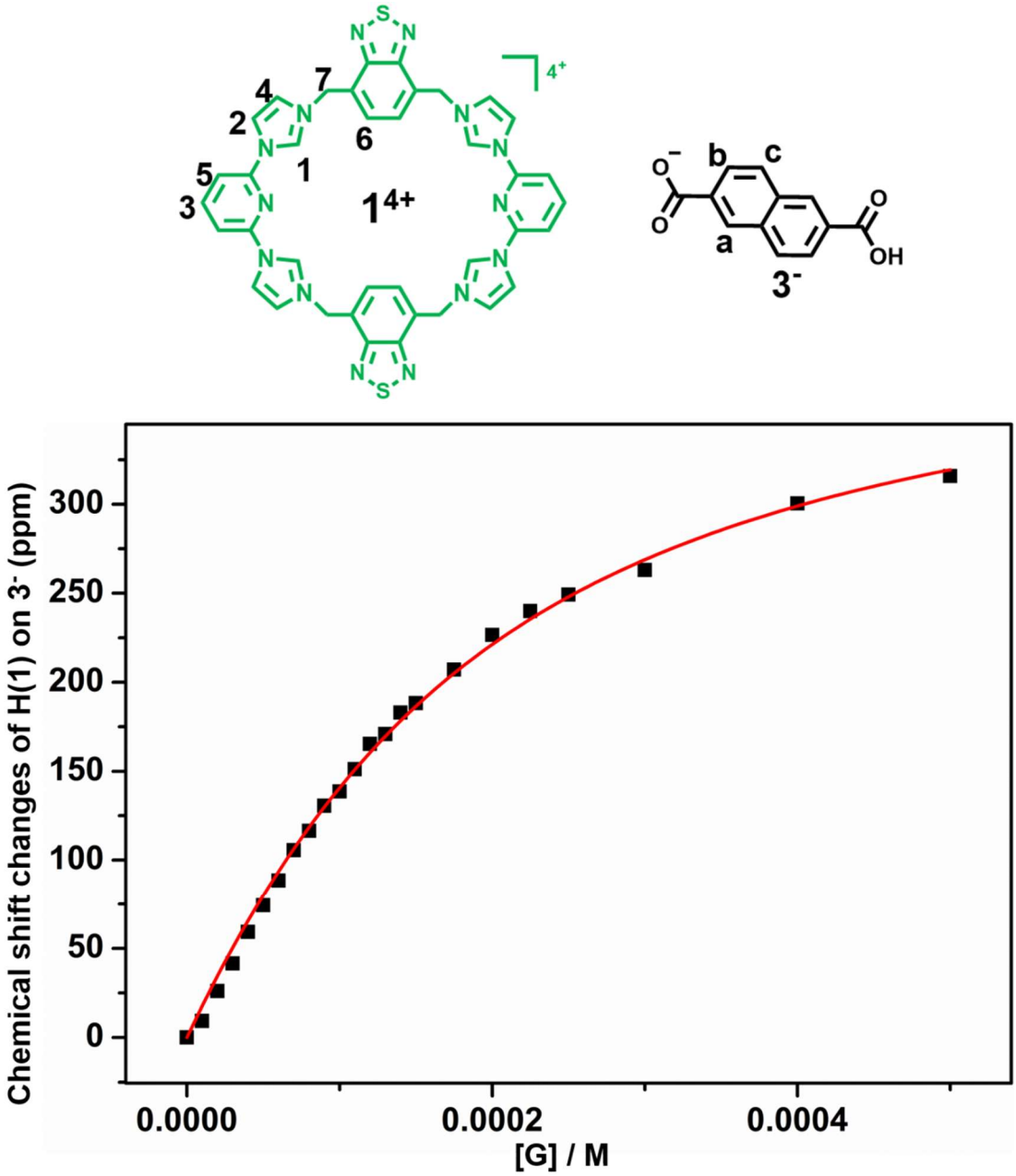

Fig. S18 ^{1}H NMR spectral binding isotherms corresponding to the interaction between $\mathbf{1}^{4+}$•4PF_6^- and 2,6'-naphthalenedicarboxylate monoanion ($\mathbf{3}^-$) in DMSO-d_6 at 298 K. The chemical shift changes of H (1) on $\mathbf{1}^{4+}$ were used for the calculation of $K_a = (7.6 \pm 0.4) \times 10^3$ M^{-1}, corresponding to the formation of the initial 1:1 complex $[\mathbf{1}^{4+}\bullet\mathbf{3}^-]^{3+}$, Fitting result based on proton 1 of $\mathbf{3}^-$.

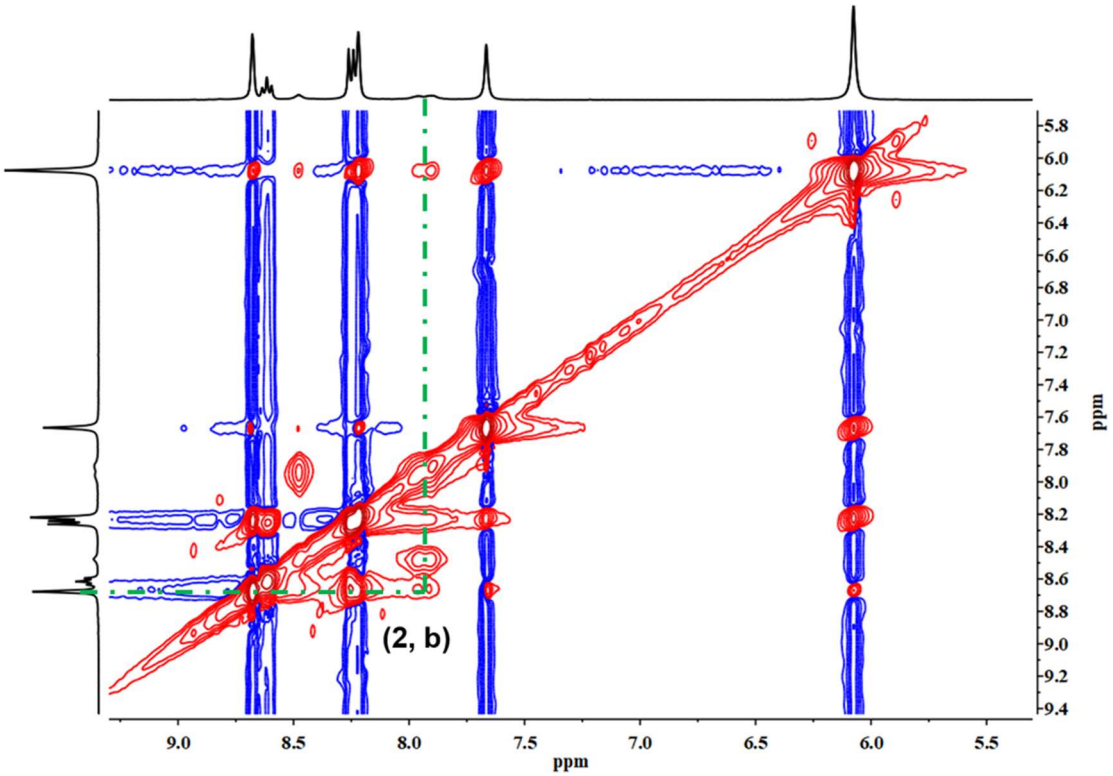

Fig. S19 NOESY spectrum of $\mathbf{1}^{4+}$•$4PF_6^-$ (10.0 mM) recorded in the presence of 1 molar equiv of $\mathbf{3}^-$ in DMSO-d_6 at 298 K. Through-space NOE was observed between H_2 on host $\mathbf{1}^{4+}$ and H_b on guest $\mathbf{3}^-$, which is taken as evidence that the host-guest interactions between macrocycle $\mathbf{1}^{4+}$ and guest anionic species $\mathbf{3}^-$.

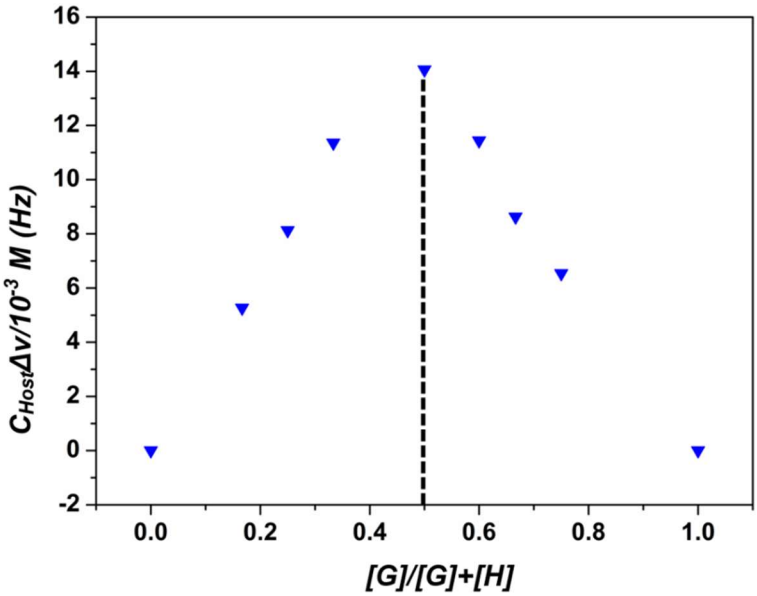

Fig. S20 ^{1}H NMR spectral Job plot corresponding to the interaction between $\mathbf{1}^{4+}$•$4PF_6^-$ and $\mathbf{3}^{2-}$ ([host] + [guest] = 1.00 mM). Maximum value was 0.5, a finding consistent with (but not a proof of) a 1:1 (host:guest) binding stoichiometry.

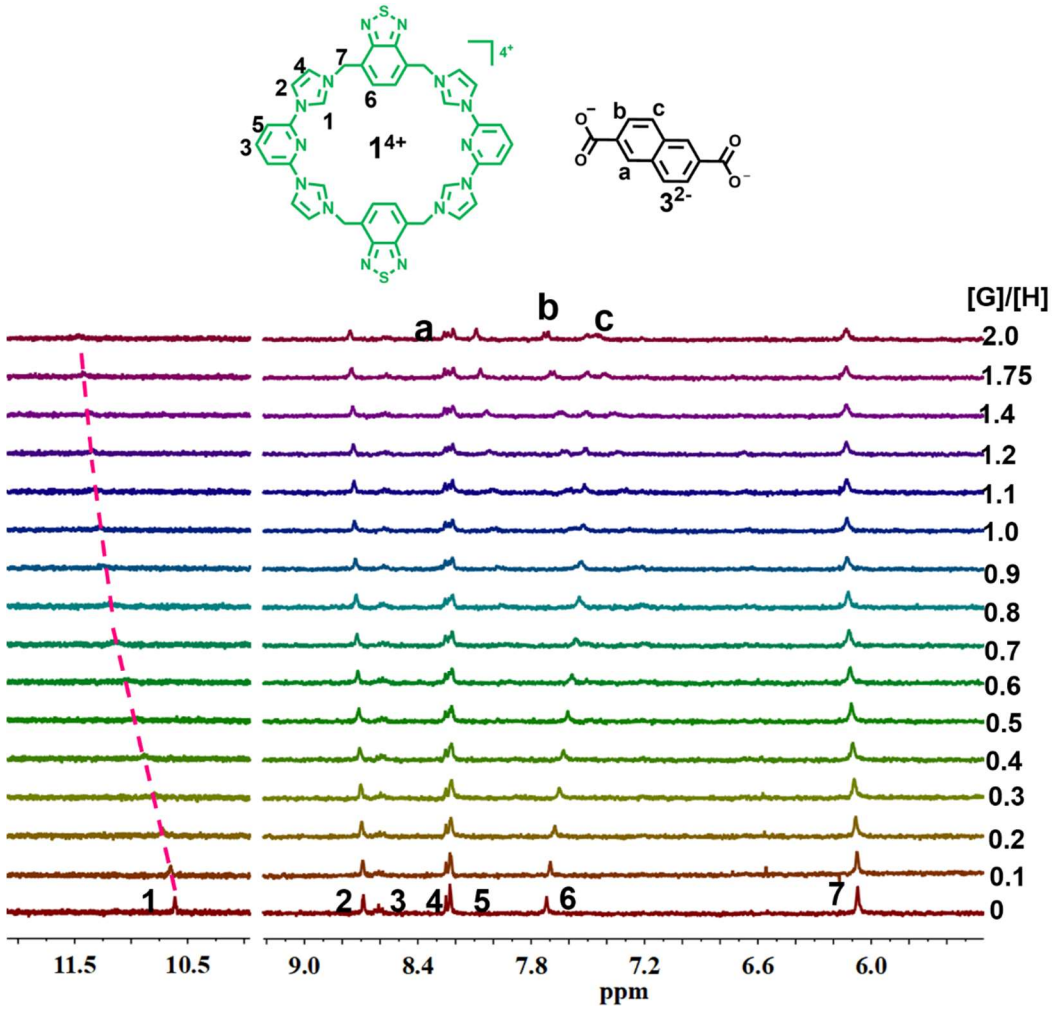

Fig. S21 400 MHz ^{1}H NMR spectroscopic titration of $\mathbf{1}^{4+}$•4PF$_6^-$ (maintained at 0.1 mM) with increasing $\mathbf{3}^{2-}$ in DMSO-d_6 at 298 K.

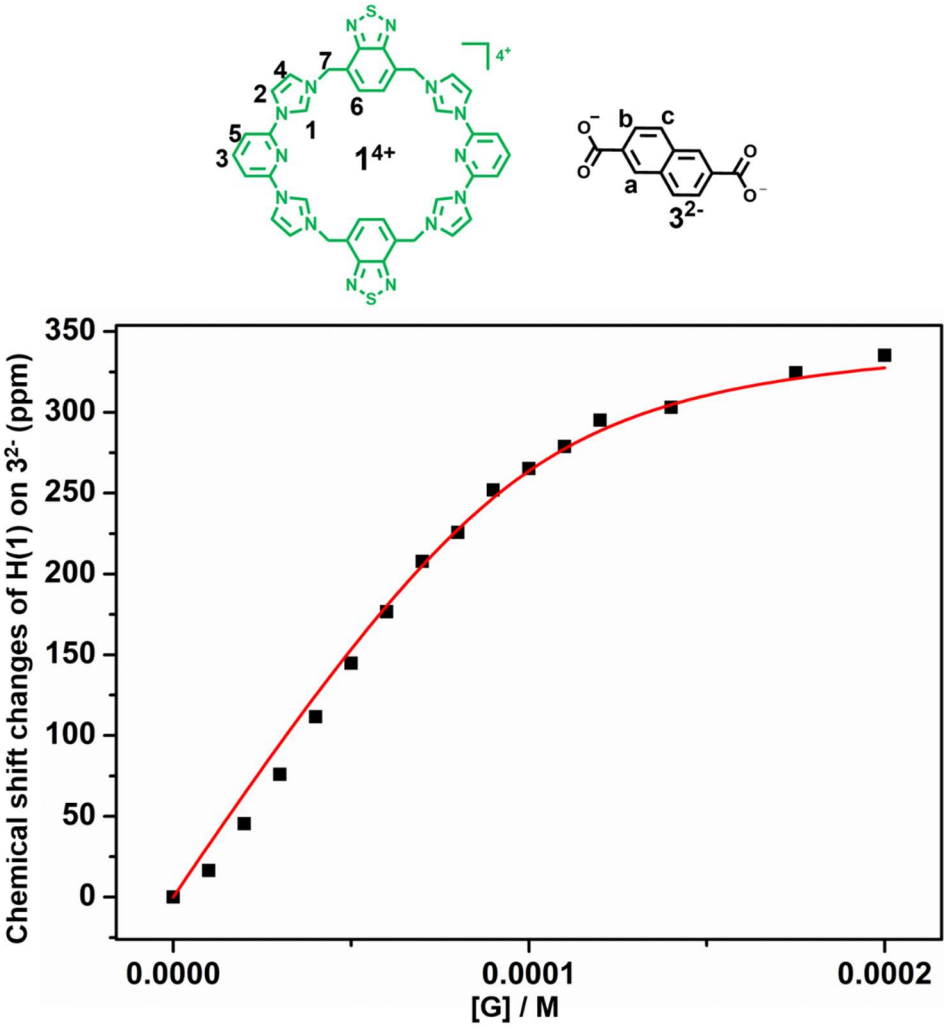

Fig. S22 ^{1}H NMR spectral binding isotherms corresponding to the interaction between $\mathbf{1}^{4+}$•4PF_6^- and $\mathbf{3}^{2-}$ in DMSO-d_6 at 298 K. The chemical shift changes of H (1) on $\mathbf{1}^{4+}$ were used for the calculation of K_a = (1.1 ± 0.4) × 10^5 M^{-1}, corresponding to the formation of the initial 1:1 complex $[\mathbf{1}^{4+}\bullet\mathbf{3}^{2-}]^{2+}$, Fitting result based on proton 1 of $\mathbf{3}^{2-}$.

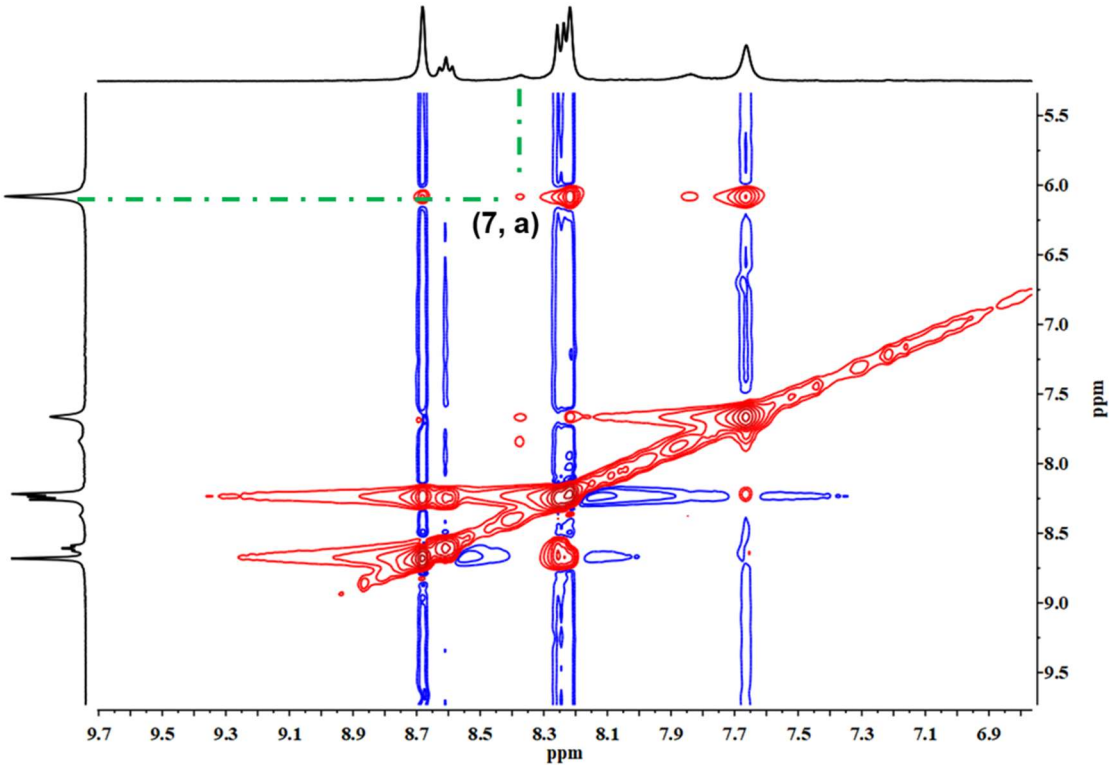

Fig. S23 NOESY spectrum of $\mathbf{1}^{4+}$•$4PF_6^-$ (10.0 mM) recorded in the presence of 1 molar equiv of $\mathbf{3}^{2-}$ in DMSO-d_6 at 298 K. Through-space NOE was observed between H_7 on host $\mathbf{1}^{4+}$ and H_a on guest $\mathbf{3}^{2-}$, which is taken as evidence that the host-guest interactions between macrocycle $\mathbf{1}^{4+}$ and guest anionic species $\mathbf{3}^{2-}$.

6. X-ray crystal data of [$\mathbf{1}^{4+}$•$\mathbf{3}^{2-}{}_2$•$10H_2O$]

X-ray crystallography of single crystal obtained by vapor diffusion of DMF (2 mL) into solutions of **2a** (5 mg) in H_2O (1 mL). CCDC number: 2299662.

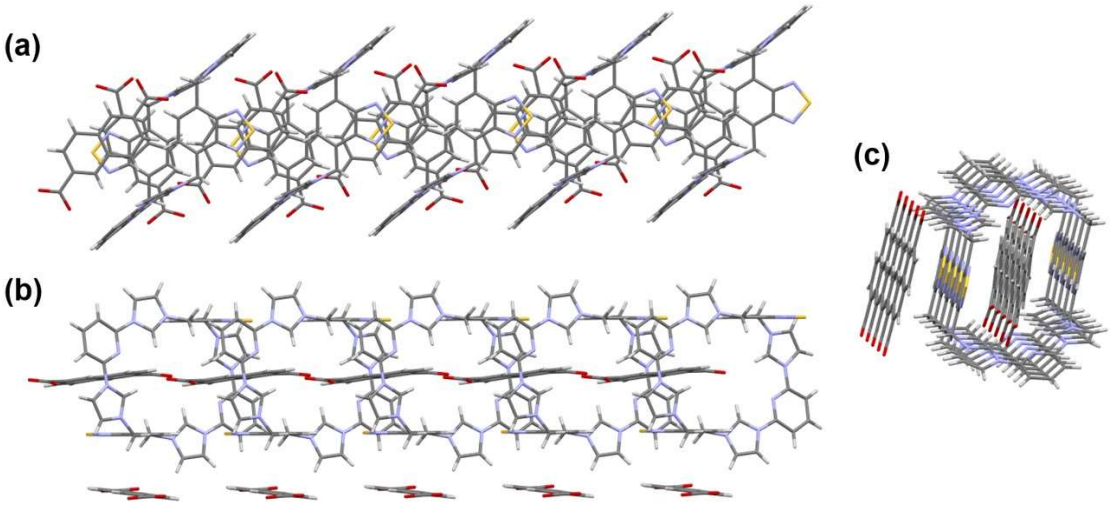

Fig. S24 Views of the 1D extended structure show assembly into [$\mathbf{1}^{4+}$•$\mathbf{3}^{2-}{}_2$•$10H_2O$]n. Solvent are omitted for clarity. Shown are top (a), front (b) and side (c) views in stick form.

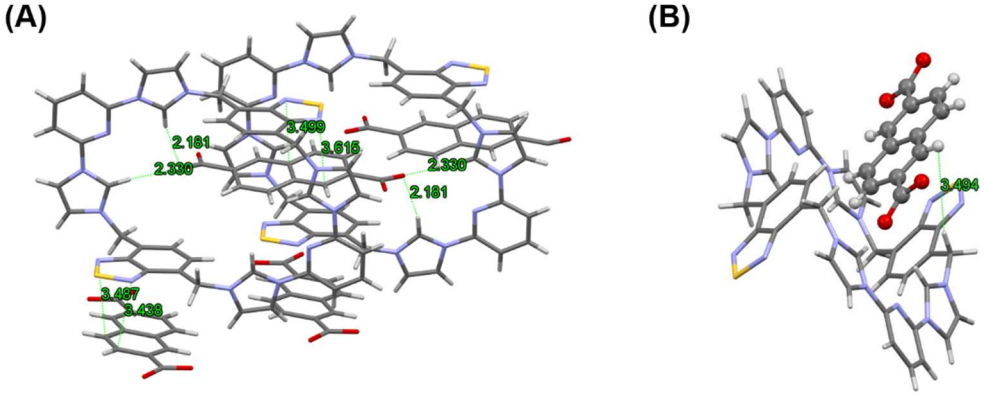

Fig. S25 (A) π-π interactions and C-H • • • O hydrogen bonds in crystal structure of [$\mathbf{1}^{4+}$•$\mathbf{3}^{2-}{}_2$•$10H_2O$]. (B) short distances (around 3.5 Å) between H_b on $\mathbf{3}^{2-}$ and H_7 on $\mathbf{1}^{4+}$.

Table S1. Crystal data and structure refinement for [$\mathbf{1}^{4+}$•$\mathbf{3}^{2-}{}_2$•$10H_2O$].

```
Bond precision:   C-C = 0.0037 A          Wavelength=1.54178

Cell:          a=8.6132(6)        b=14.1366(11)     c=15.1958(12)
               alpha=103.568(5)   beta=105.921(4)   gamma=102.220(4)
Temperature:   223 K

                Calculated                  Reported
Volume          1652.5(2)                   1652.5(2)
Space group     P -1                        P -1
Hall group      -P 1                        -P 1
                C38 H30 N14 S2, 2(C12 H6
Moiety formula  O4), 8(H2 O), 2(O) [+       ?
                solvent]
                C62 H58 N14 O18 S2 [+
Sum formula     solvent]                    C62 H62 N14 O18 S2
Mr              1351.34                     1355.37
Dx,g cm-3       1.358                       1.362
Z               1                           1
Mu (mm-1)       1.419                       1.419
F000            704.0                       708.0
F000'           706.97
h,k,lmax        10,17,18                    10,17,18
Nref            6566                        6539
Tmin,Tmax       0.775,0.868                 0.671,0.774
Tmin'           0.775

Correction method= # Reported T Limits: Tmin=0.671 Tmax=0.774
AbsCorr = MULTI-SCAN

Data completeness= 0.996           Theta(max)= 72.488
R(reflections)= 0.0519( 5092)                          wR2(reflections)=
                                                       0.1452( 6539)
S = 1.023                  Npar= 481
```

7. Chemical fuels for molecular switch

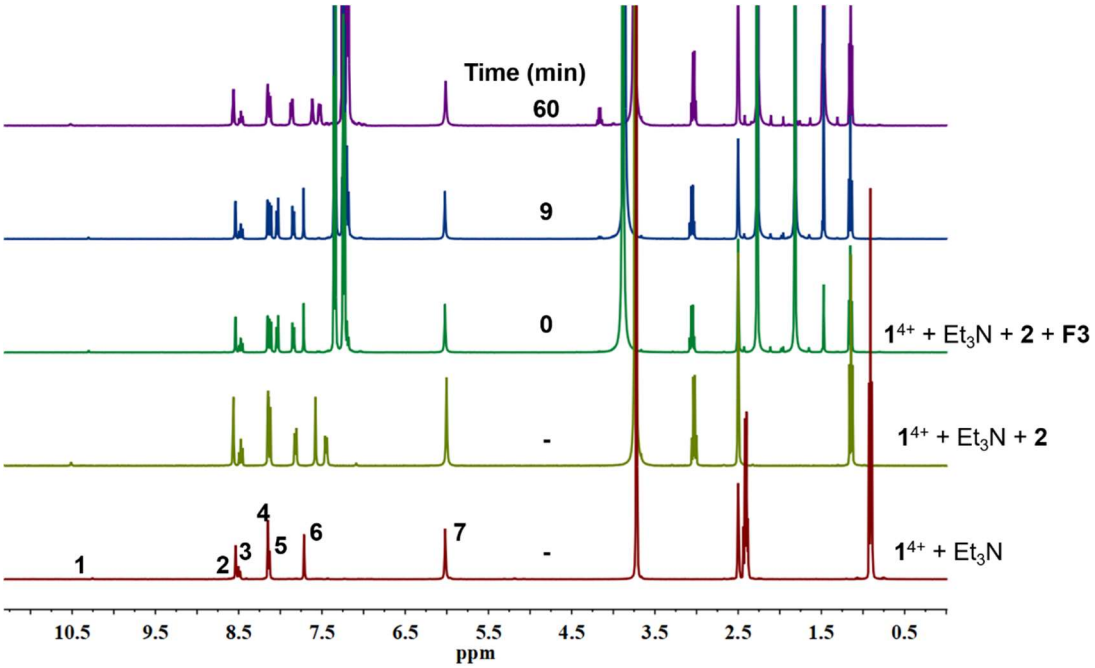

Fig. S26 Full time dependent ^{1}H NMR spectroscopic changes of **F3** (125 mM) in DMSO-d_6/D_2O (9/1, v/v) at 303 K (400 MHz) observed after applying one pulse of chemical fuel **F3**.

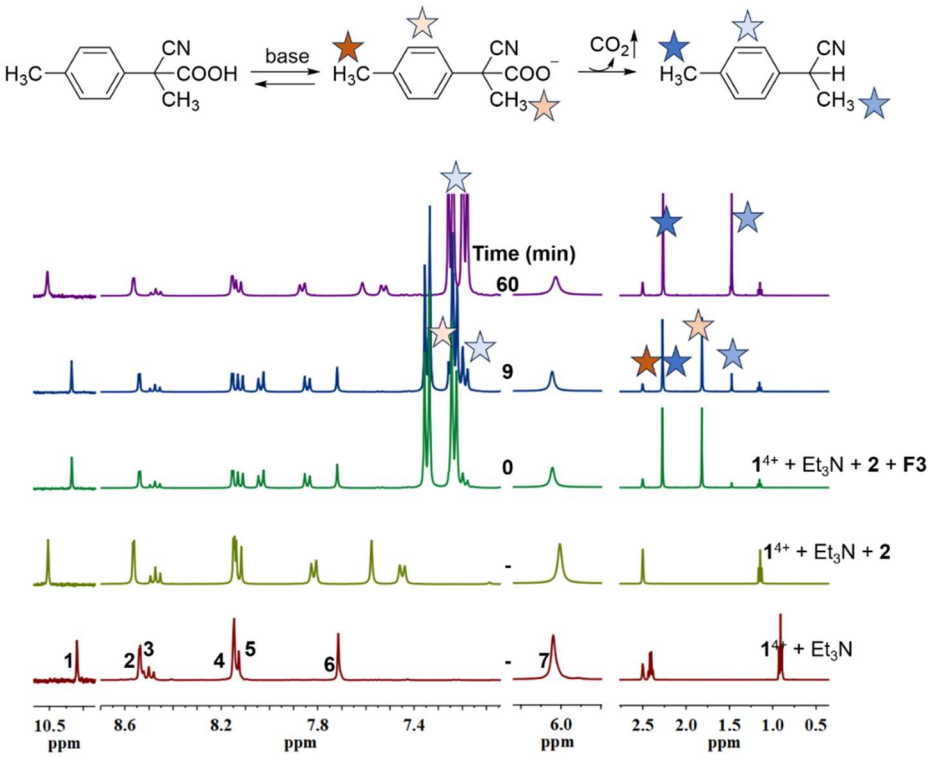

Fig. S27 Partial time dependent ^{1}H NMR spectroscopic changes of **F3** (125 mM) in DMSO-d_6/D_2O (9/1, v/v) at 298 K (400 MHz) observed after applying one pulse of chemical fuel **F3**.

Controlling the duration of molecular switching of the [$\mathbf{1}^{4+}$•$\mathbf{2}^{2-}$]→[$\mathbf{1}^{4+}$ + **2**]→[$\mathbf{1}^{4+}$•$\mathbf{2}^{2-}$] by regulating the fuel **F1** - **F5.**

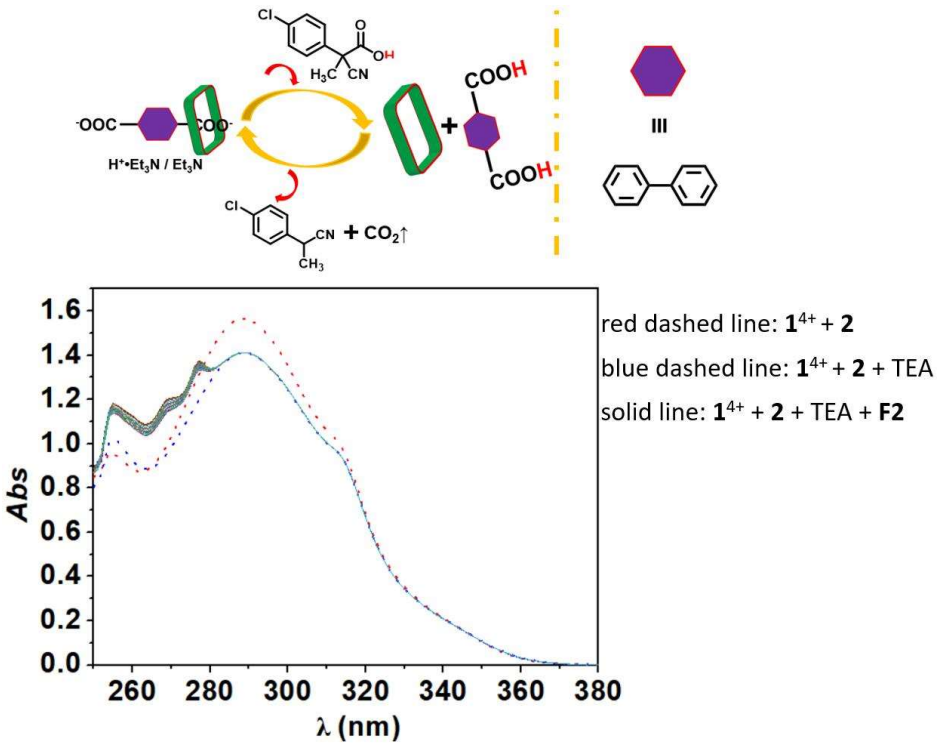

Fig. S28 Time dependent UV-vis spectra changes seen for $\mathbf{2}^{2-}$ (0.03 mM) created via mixing **2** (0.06 μmol, 0.03 mM) and Et_3N (0.3 μmol) in DMSO/H_2O (9/1, v/v) at 298 K observed in the presence of $\mathbf{1}^{4+}$ after applying one pulse of **F2** (1.5 μmol).

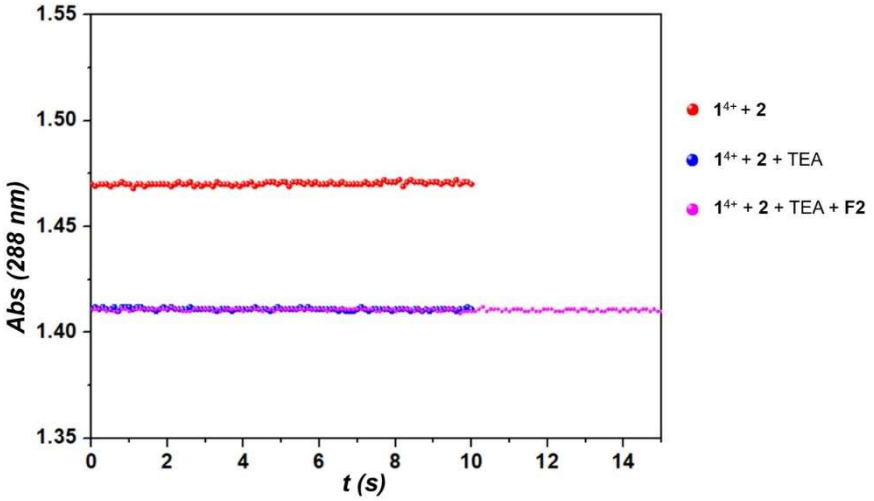

Fig. S29 Time dependent of the absorbance value at 288 nm changes (in a 0.1 second interval) seen for $\mathbf{2}^{2-}$ (0.03 mM) created via mixing **2** (0.06 μmol, 0.03 mM) and Et_3N (0.3 μmol) in DMSO/H_2O (9/1, v/v) at 298 K observed in the presence of $\mathbf{1}^{4+}$ after applying one pulse of **F2** (1.5 μmol).

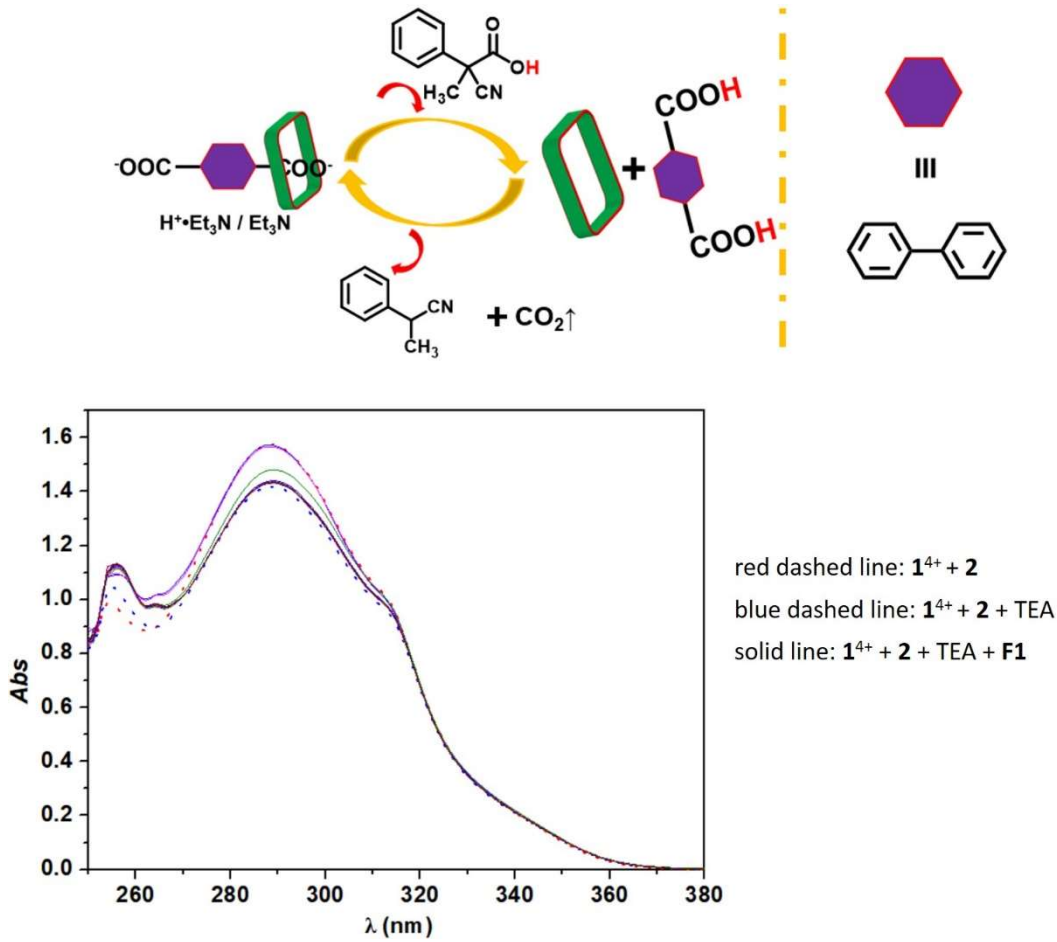

Fig. S30 Time dependent UV-vis spectra changes seen for $\mathbf{2}^{2-}$ (0.03 mM) created via mixing **2** (0.06 μmol, 0.03 mM) and Et_3N (0.3 μmol) in DMSO/H_2O (9/1, v/v) at 298 K observed in the presence of $\mathbf{1}^{4+}$ after applying one pulse of **F1** (1.5 μmol).

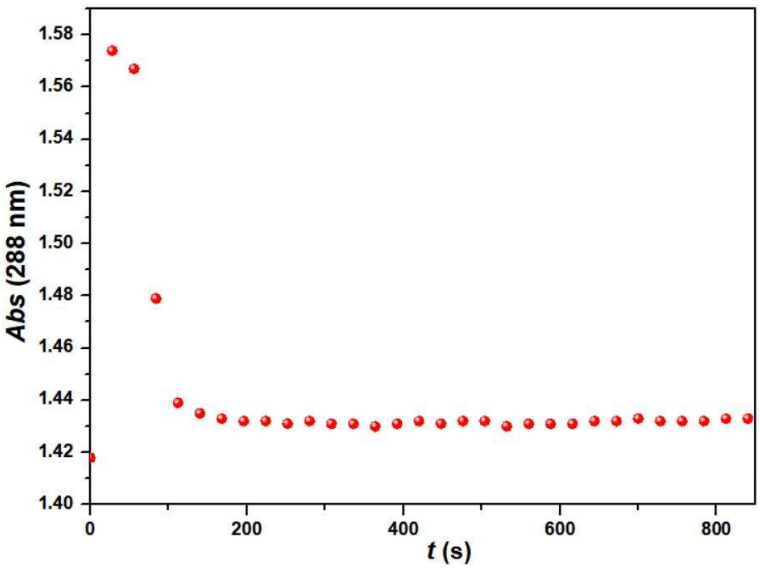

Fig. S31 absorbance *vs*. time profiles of the reaction mixtures composed of $\mathbf{1}^{4+}$, **2** and Et_3N after applying one pulse of chemical fuel **F1** (red trace).

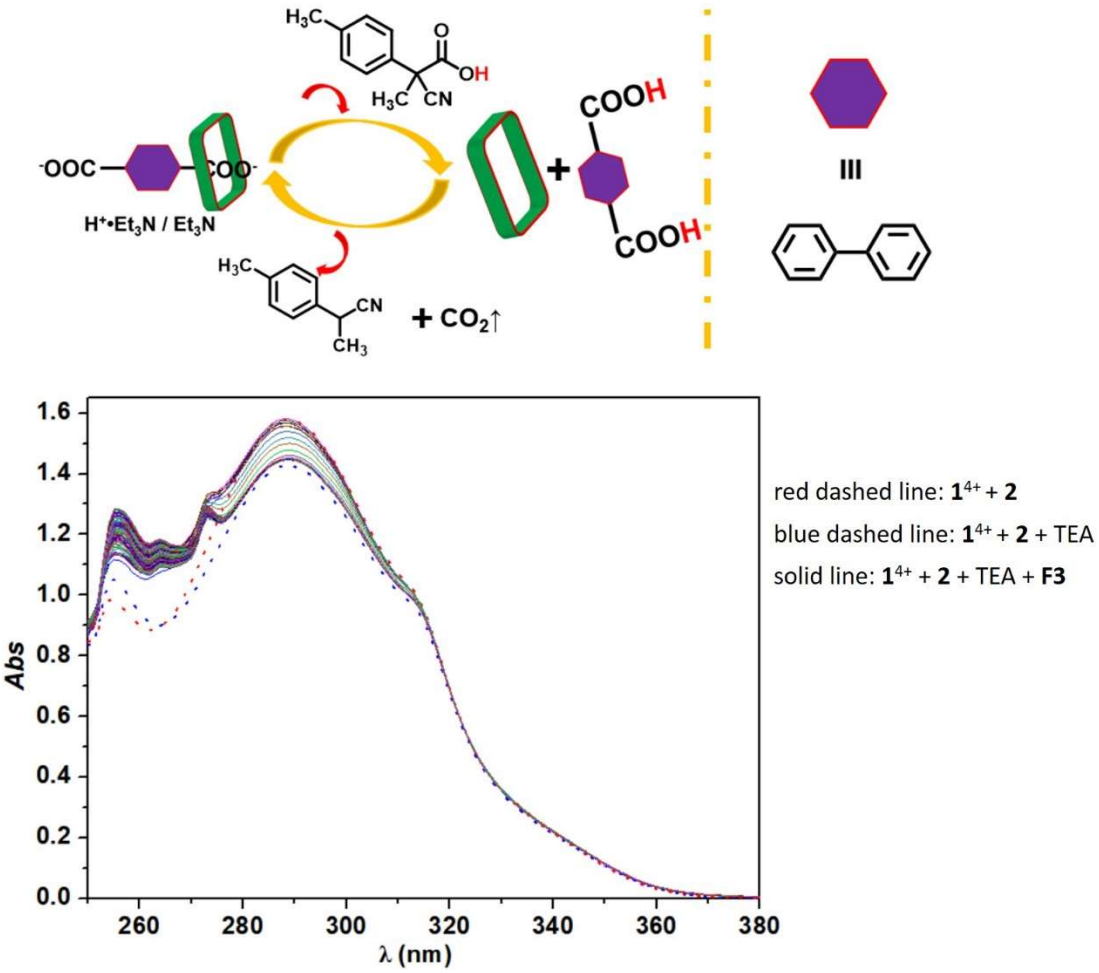

Fig. S32 Time dependent UV-vis spectra changes seen for $\mathbf{2}^{2-}$ (0.03 mM) created via mixing **2** (0.06 μmol, 0.03 mM) and Et_3N (0.3 μmol) in DMSO/H_2O (9/1, v/v) at 298 K observed in the presence of $\mathbf{1}^{4+}$ after applying one pulse of **F3** (1.5 μmol).

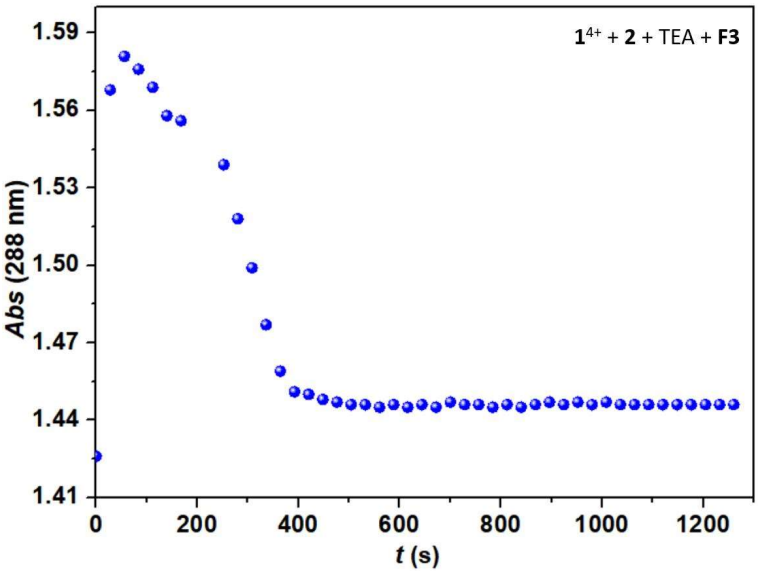

Fig. S33 absorbance *vs*. time profiles of the reaction mixtures composed of $\mathbf{1}^{4+}$, **2** and Et_3N after applying one pulse of chemical fuel **F3** (blue trace).

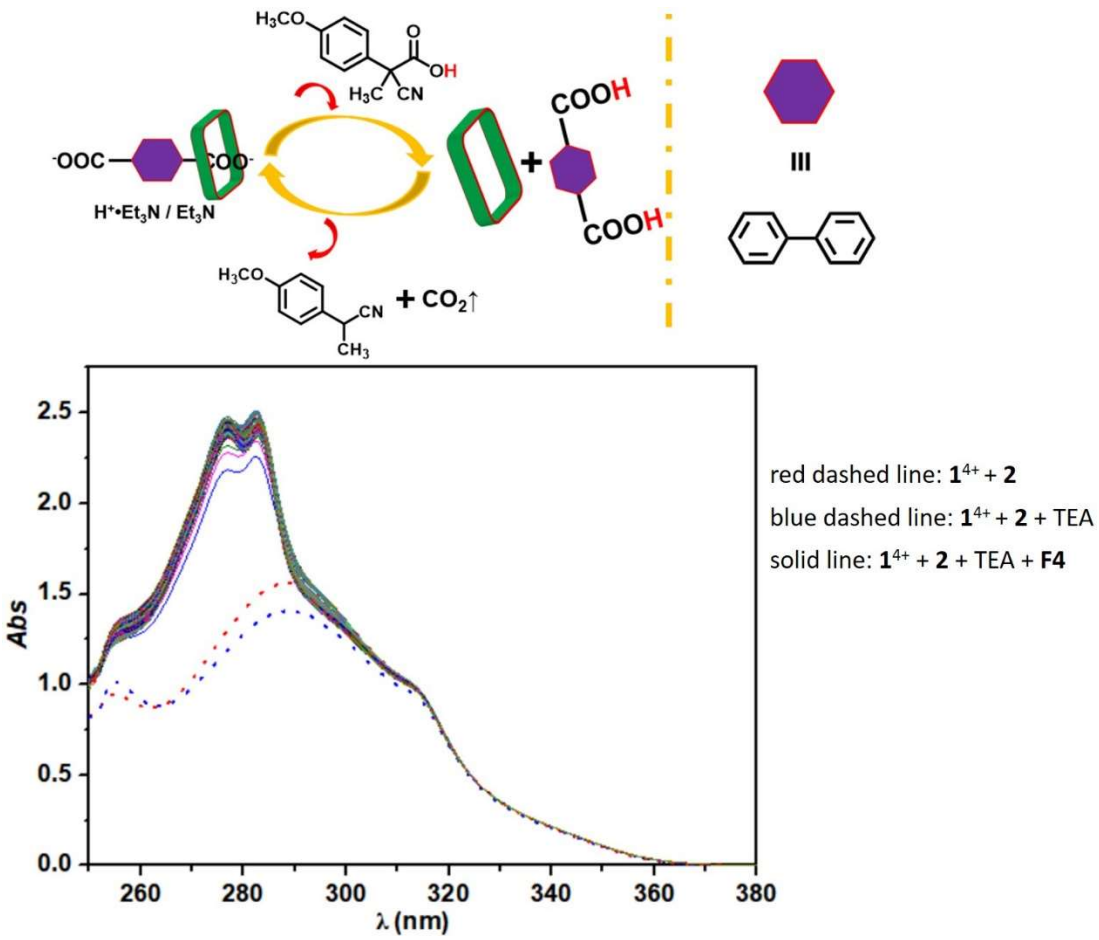

Fig. S34 Time dependent UV-vis spectra changes seen for $\mathbf{2}^{2-}$ (0.03 mM) created via mixing **2** (0.06 μmol, 0.03 mM) and Et_3N (0.3 μmol) in DMSO/H_2O (9/1, v/v) at 298 K observed in the presence of $\mathbf{1}^{4+}$ after applying one pulse of **F4** (1.5 μmol).

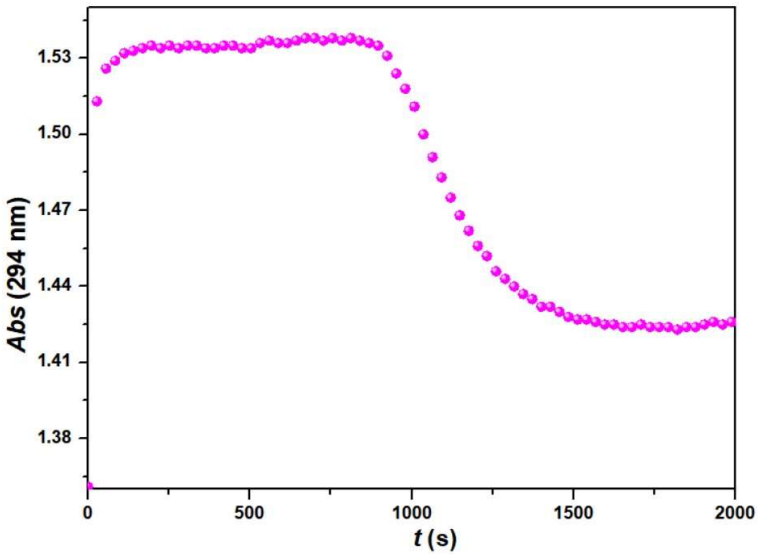

Fig. S35 Absorbance *vs*. time profiles of the reaction mixtures composed of $\mathbf{1}^{4+}$, **2** and Et_3N after applying one pulse of chemical fuel **F4** (pink trace).

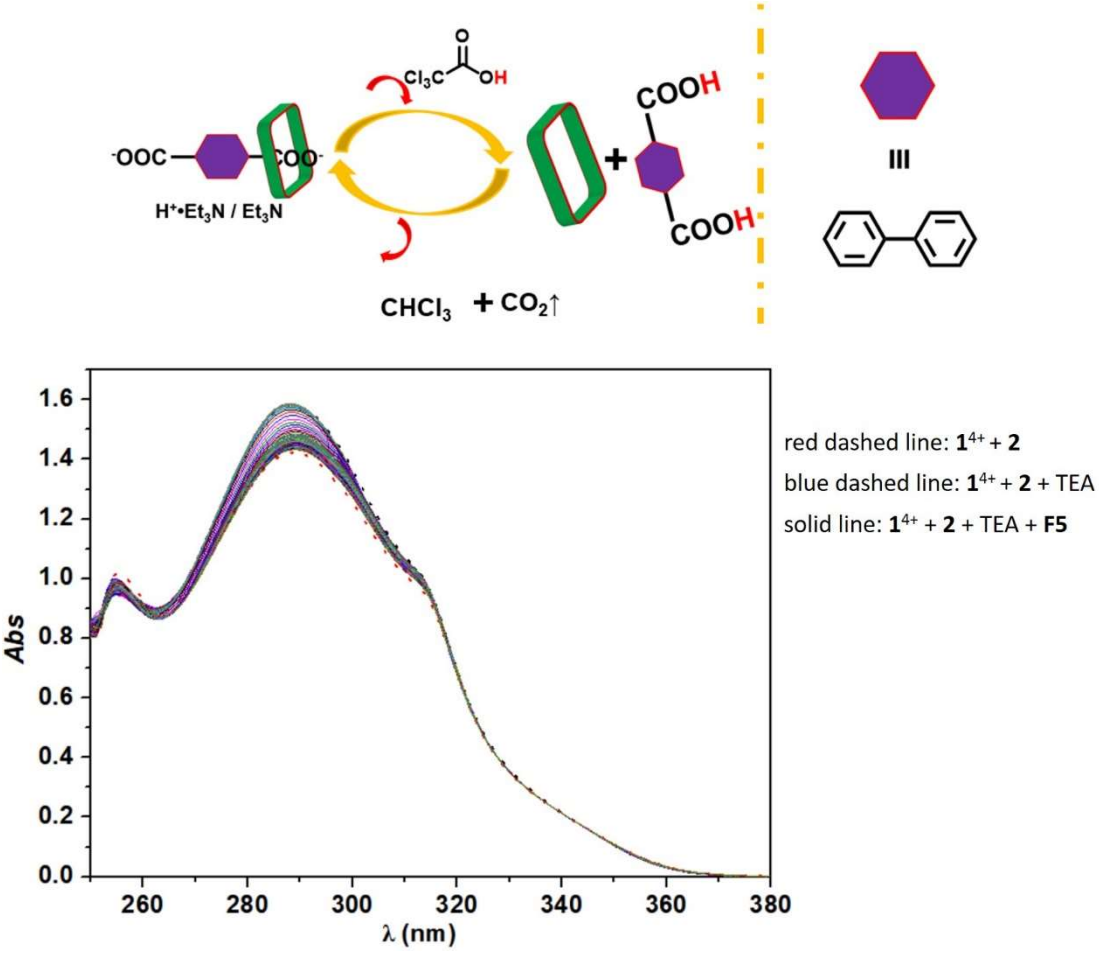

Fig. S36 Time dependent UV-vis spectra changes seen for $\mathbf{2}^{2-}$ (0.03 mM, created via mixing 4,4'-biphenyldicarboxylic acid (**2**) (0.06 μmol, 0.03 mM) and Et_3N (0.3 μmol) in DMSO/H_2O (9/1, v/v) at 298 K observed in the presence of $\mathbf{1}^{4+}$ after applying one pulse of chemical fuel (**F5**; 1.5 μmol).

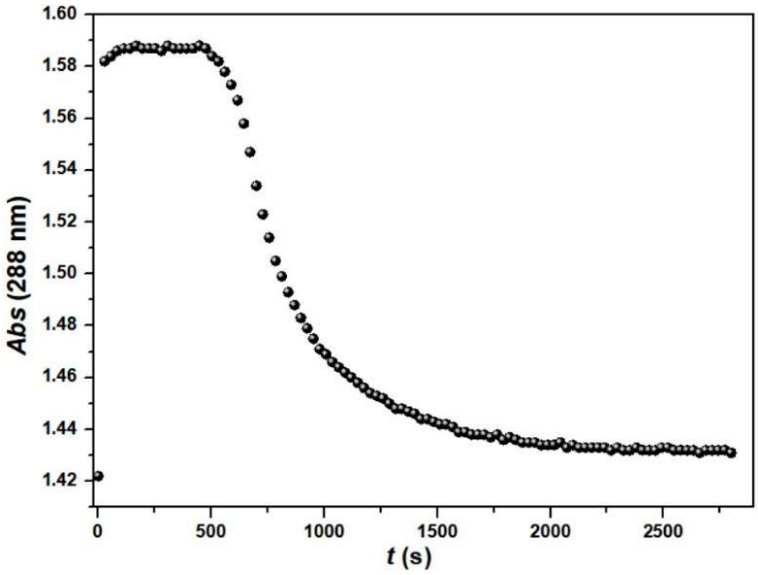

Fig. S37 absorbance *vs*. time profiles of the reaction mixtures composed of $\mathbf{1}^{4+}$, **2** and Et_3N after applying one pulse of chemical fuel **F5** (black trace).

Controlling the duration of molecular switching of the [$\mathbf{1}^{4+}$•$\mathbf{3}^{2-}$]→[$\mathbf{1}^{4+}$ + **3**]→[$\mathbf{1}^{4+}$•$\mathbf{3}^{2-}$] by regulating the fuel **F1** - **F5**.

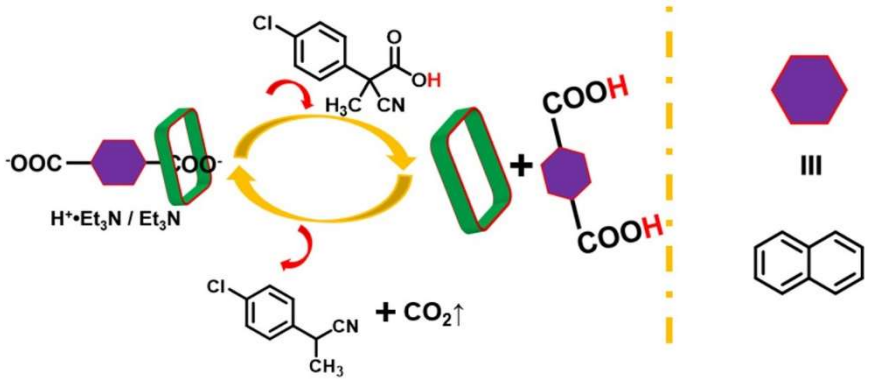

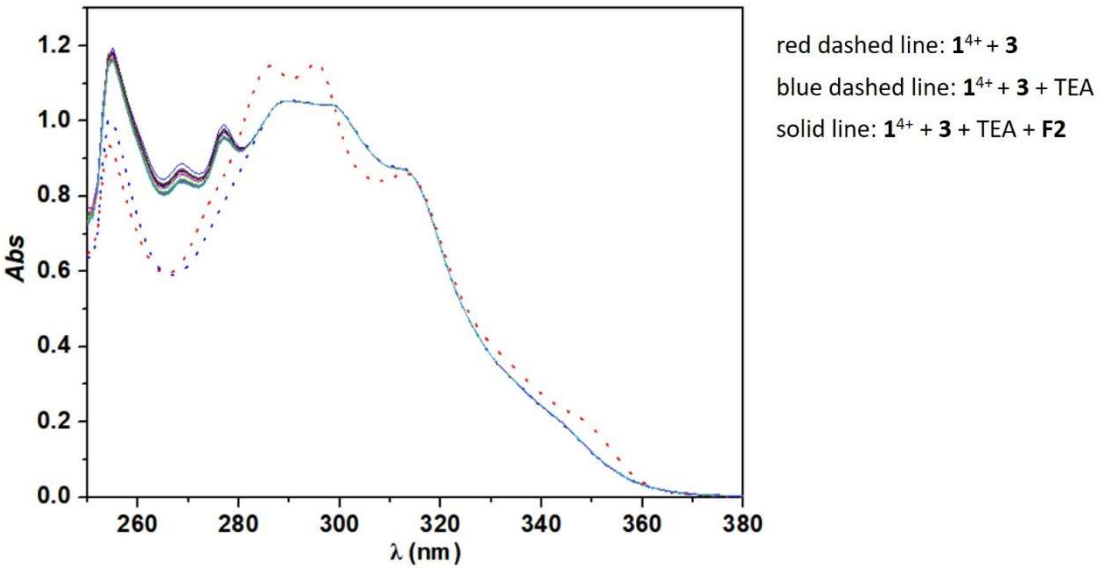

Fig. S38. Time dependent UV-vis spectra changes seen for $\mathbf{3}^{2-}$ (0.03 mM, created via mixing **3** (0.06 μmol, 0.03 mM) and Et_3N (0.3 μmol) in DMSO/H_2O (9/1, v/v) at 298 K observed in the presence of $\mathbf{1}^{4+}$ after applying one pulse of **F2** (1.5 μmol).

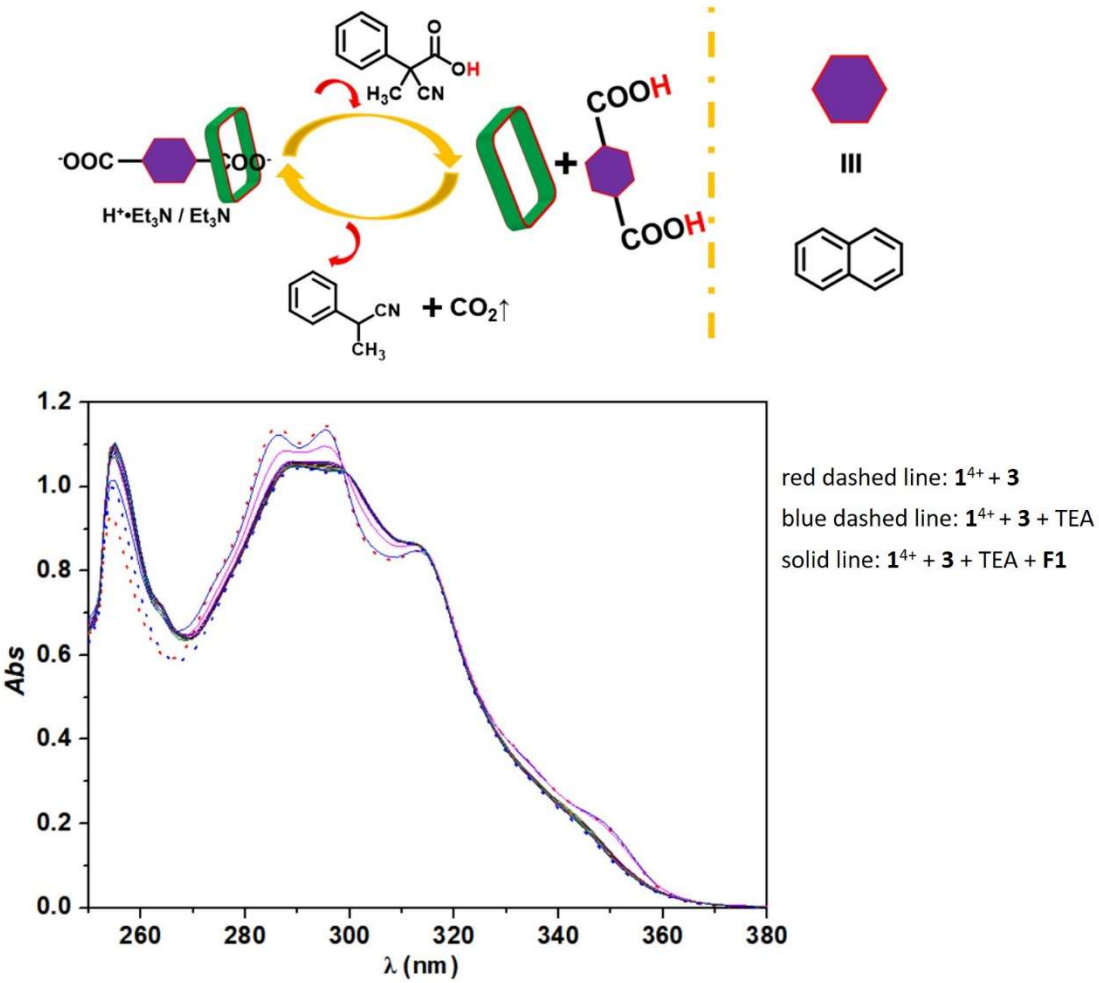

Fig. S39. Time dependent UV-vis spectra changes seen for $\mathbf{3}^{2-}$ (0.03 mM, created via mixing **3** (0.06 µmol, 0.03 mM) and Et_3N (0.3 µmol) in DMSO/H_2O (9/1, v/v) at 298 K observed in the presence of $\mathbf{1}^{4+}$ after applying one pulse of **F1** (1.5 µmol).

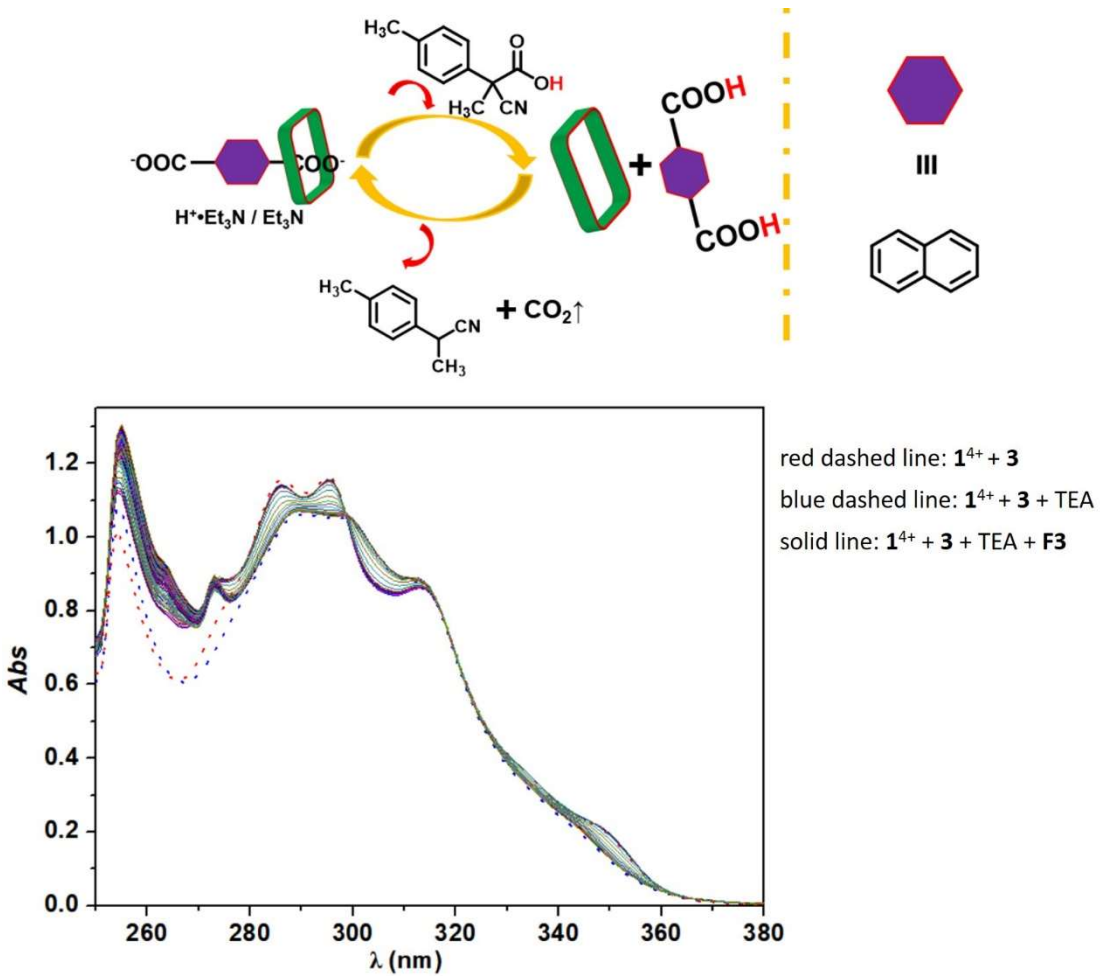

Fig. S40. Time dependent UV-vis spectra changes seen for $\mathbf{3}^{2-}$ (0.03 mM, created via mixing **3** (0.06 µmol, 0.03 mM) and Et_3N (0.3 µmol) in DMSO/H_2O (9/1, v/v) at 298 K observed in the presence of $\mathbf{1}^{4+}$ after applying one pulse of **F3** (1.5 µmol).

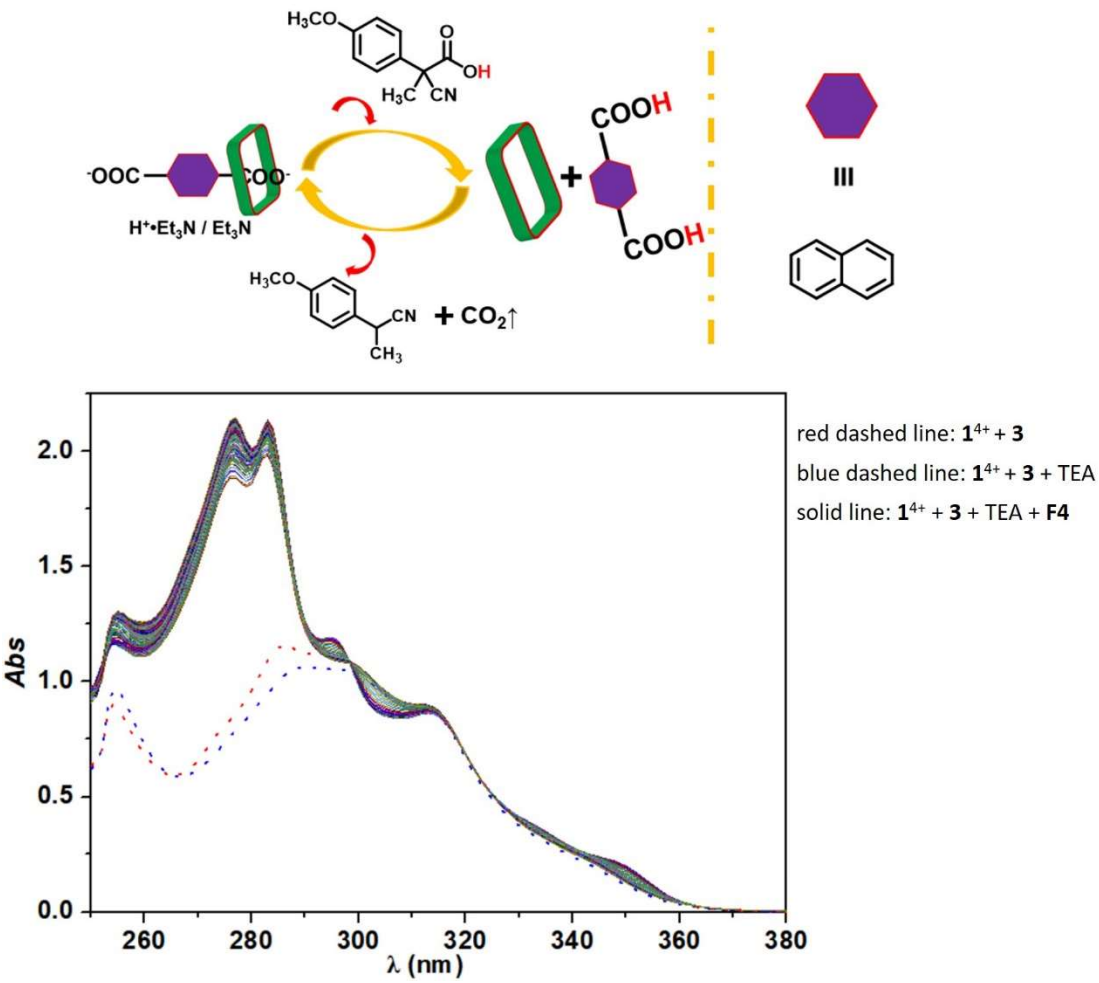

Fig. S41 Time dependent UV-vis spectra changes seen for $\mathbf{3}^{2-}$ (0.03 mM, created via mixing **3** (0.06 µmol, 0.03 mM) and Et_3N (0.3 µmol) in DMSO/H_2O (9/1, v/v) at 298 K observed in the presence of $\mathbf{1}^{4+}$ after applying one pulse of **F4** (1.5 µmol).

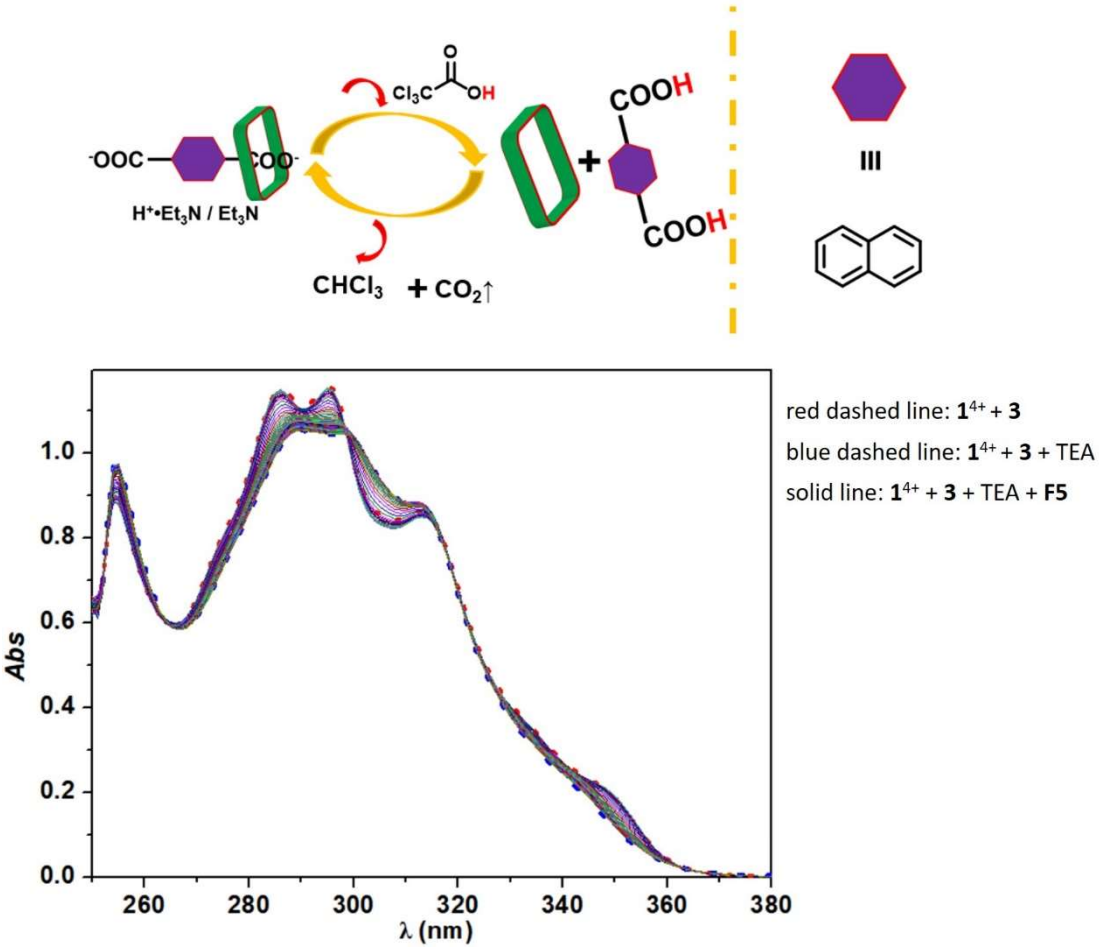

Fig. S42 Time dependent UV-vis spectra changes seen for $\mathbf{3}^{2-}$ (0.03 mM, created via mixing **3** (0.06 μmol, 0.03 mM) and Et_3N (0.3 μmol) in DMSO/H_2O (9/1, v/v) at 298 K observed in the presence of $\mathbf{1}^{4+}$ after applying one pulse of **F5** (1.5 μmol).

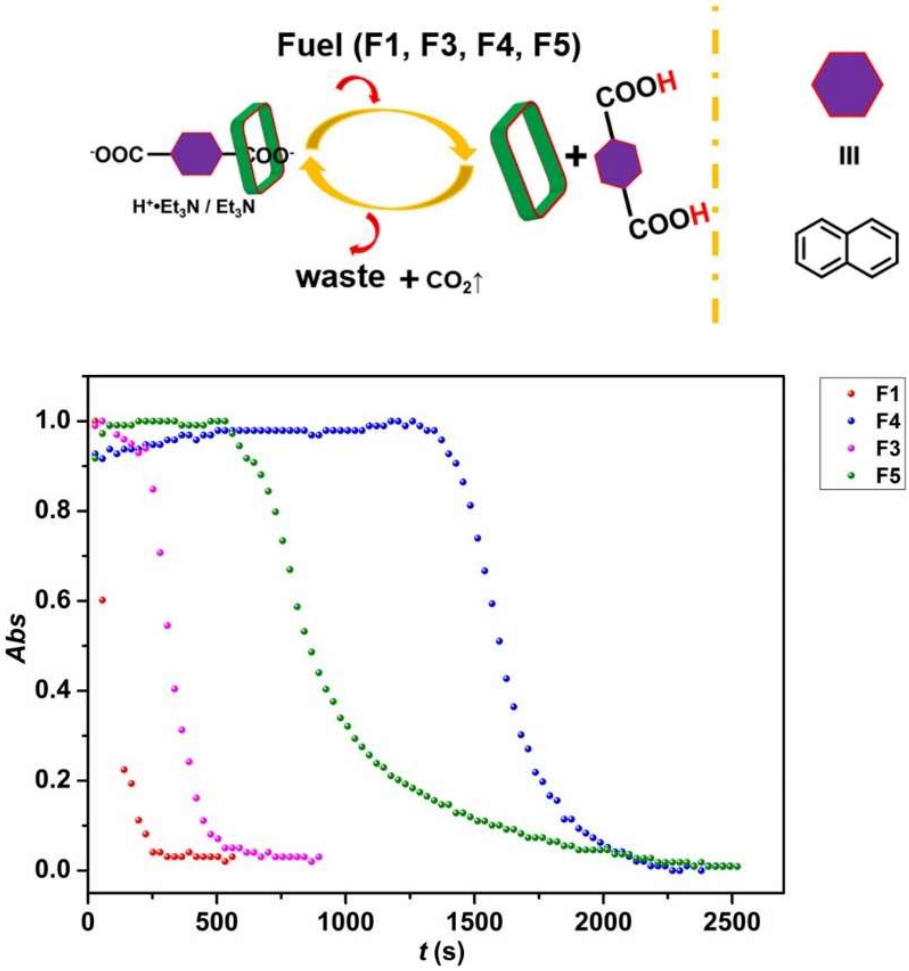

Fig. S43 absorbance *vs*. time profiles of the reaction mixtures composed of $\mathbf{1}^{4+}$, **3** and Et_3N after applying one pulse of chemical fuel **F1**(red trace), **F3**(pink trace), **F4**(blue trace), **F5**(green trace), respectively. The data from the summary of figures S38-S41.

Controlling the duration of molecular switching of the [$\mathbf{1}^{4+}$•$\mathbf{2}^{2-}$]→[$\mathbf{1}^{4+}$ + **2**]→[$\mathbf{1}^{4+}$•$\mathbf{2}^{2-}$] by regulating the amount of the chemical fuel.

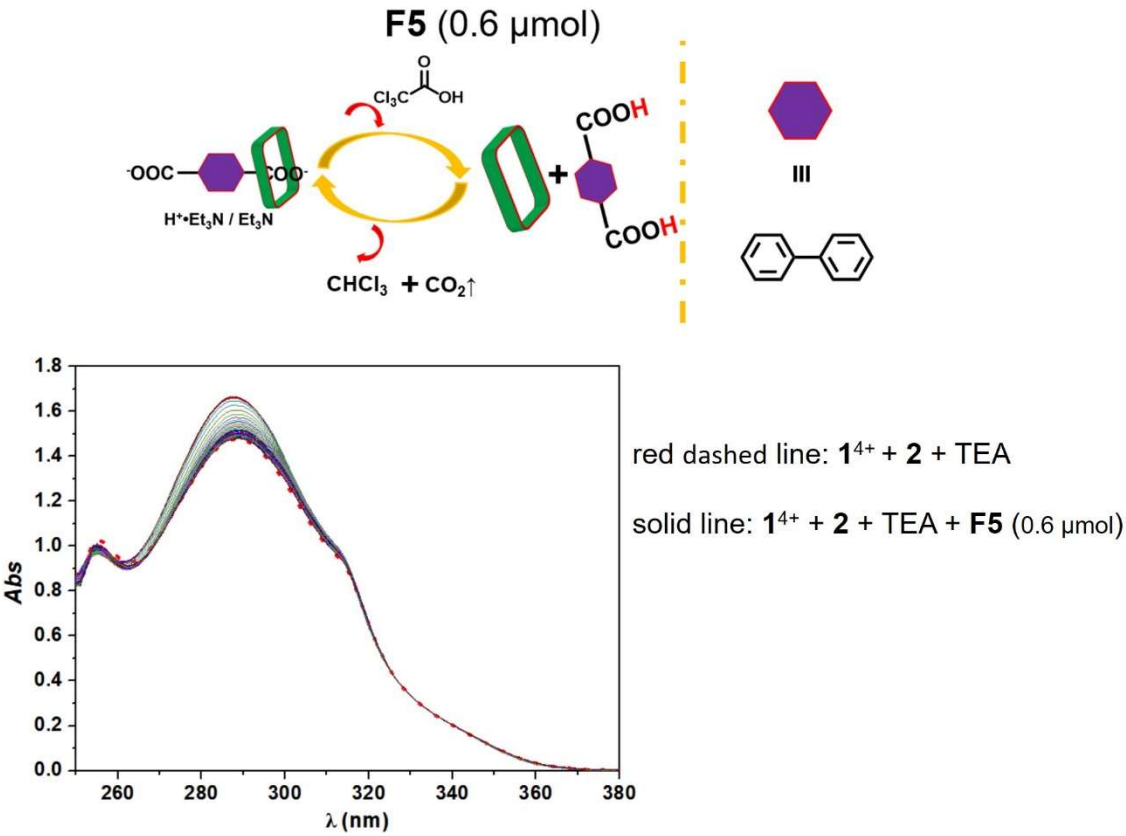

Fig. S44. Time dependent UV-vis spectra changes seen for $\mathbf{2}^{2-}$ (0.03 mM, created via mixing **2** (0.06 μmol, 0.03 mM) and Et_3N (0.3 μmol) in DMSO/H_2O (9/1, v/v) at 298 K observed in the presence of $\mathbf{1}^{4+}$ after applying one pulse of **F5** (0.6 μmol).

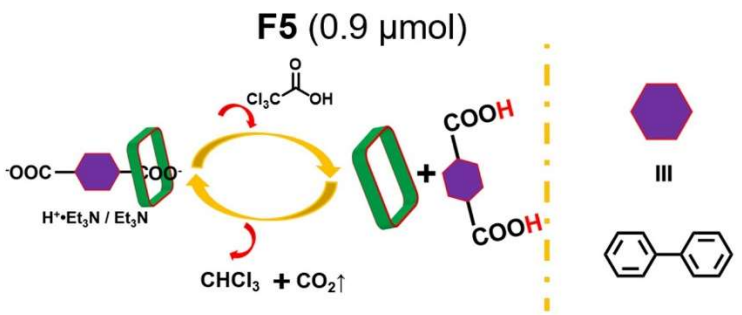

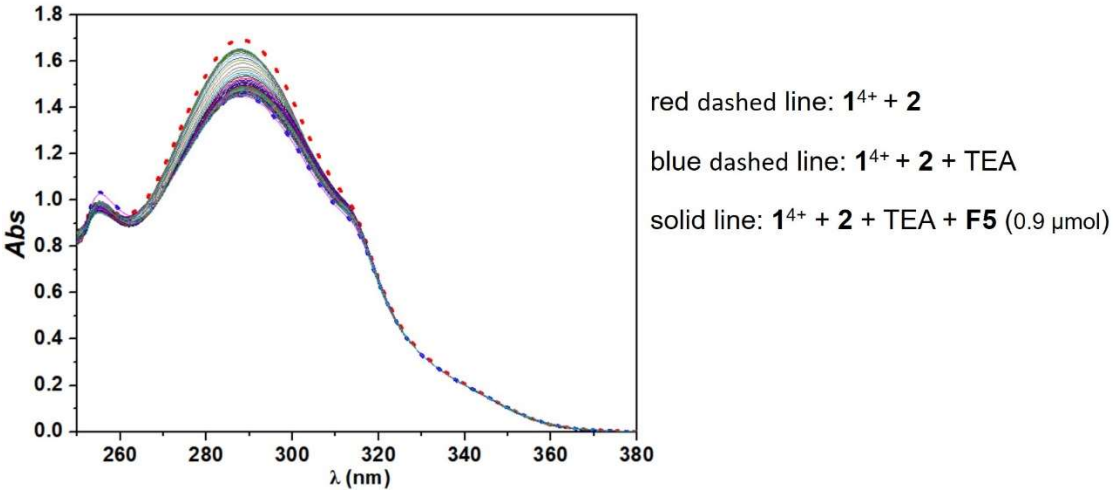

Fig. S45 Time dependent UV-vis spectra changes seen for $\mathbf{2}^{2-}$ (0.03 mM, created via mixing **2** (0.06 μmol, 0.03 mM) and Et_3N (0.3 μmol) in DMSO/H_2O (9/1, v/v) at 298 K observed in the presence of $\mathbf{1}^{4+}$ after applying one pulse of **F5** (0.9 μmol).

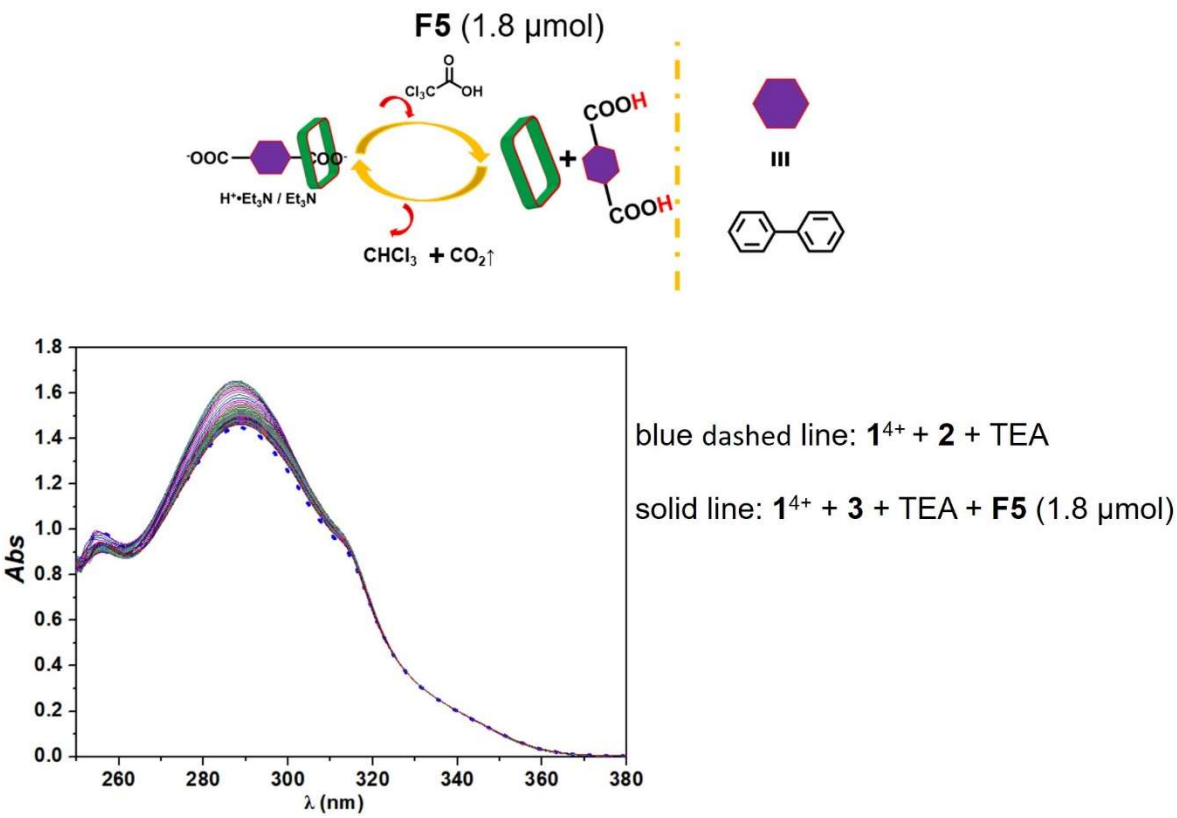

Fig. S46 Time dependent UV-vis spectra changes seen for $\mathbf{2}^{2-}$ (0.03 mM, created via mixing **3** (0.06 μmol, 0.03 mM) and Et_3N (0.3 μmol) in DMSO/H_2O (9/1, v/v) at 298 K observed in the presence of $\mathbf{1}^{4+}$ after applying one pulse of **F5** (1.8 μmol).

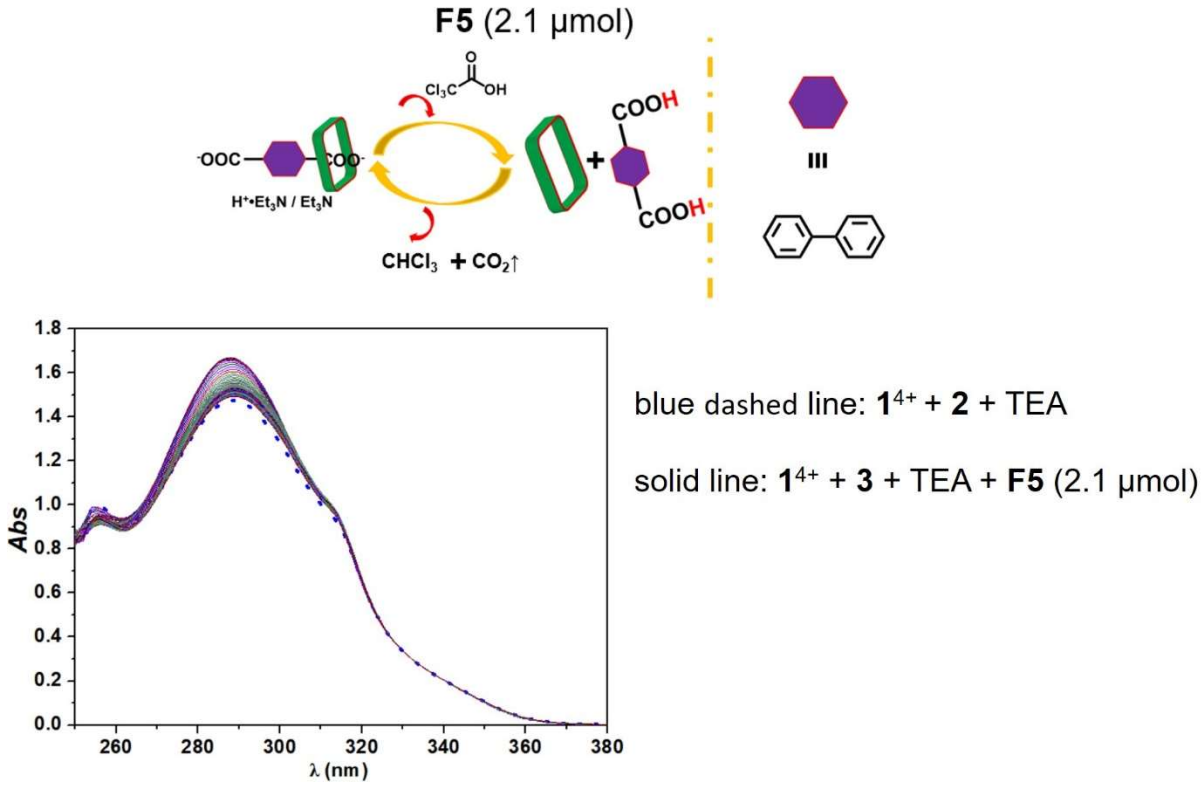

Fig. S47 Time dependent UV-vis spectra changes seen for $\mathbf{2}^{2-}$ (0.03 mM, created via mixing **3** (0.06 μmol, 0.03 mM) and Et_3N (0.3 μmol) in DMSO/H_2O (9/1, v/v) at 298 K observed in the presence of $\mathbf{1}^{4+}$ after applying one pulse of **F5** (2.1 μmol).

8. The fuel-driven reversible cycle of molecular switch

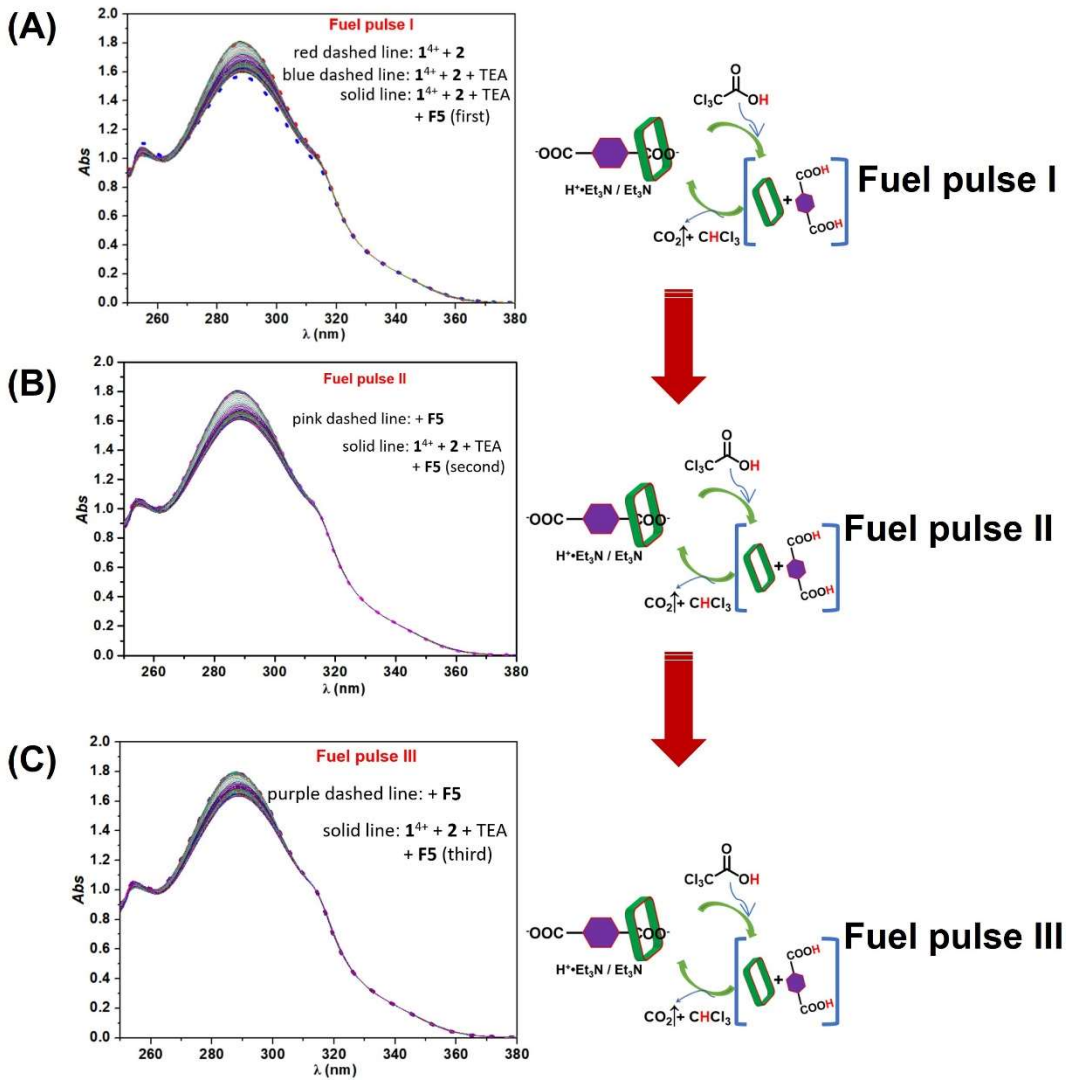

Fig. S48 (A) Time dependent UV-vis spectra changes seen for $\mathbf{2}^{2-}$ (0.03 mM, created via mixing **3** (0.06 μmol, 0.03 mM) and Et_3N (0.3 μmol) in DMSO/H_2O (9/1, v/v) at 298 K observed in the presence of $\mathbf{1}^{4+}$ after applying one pulse of **F5** (1.5 μmol). The spectra pictured as red broken lines refer to the reaction mixtures composed of $\mathbf{1}^{4+}$ and **2**. The spectra pictured as blue broken lines refer to the reaction mixtures composed of $\mathbf{1}^{4+}$, **2** and Et_3N; the spectra pictured as full lines refer to the reaction mixtures composed of $\mathbf{1}^{4+}$, **2**, Et_3N and **F5** as time goes on; (B) Time dependent UV-vis spectra changes seen for the reaction mixtures in Fig. S48(A) after continuing treatment with one pulse of **F5** (1.5 μmol); (C) Time dependent UV-vis spectra changes seen for the reaction mixtures in Fig. S48(B) after continuing treatment with one pulse of **F5** (1.5 μmol).

9. Molecular modeling

Geometries of molecules were optimized at B3LYP/6-31+G(d) level with Grimme's dispersion correction followed by frequency calculations to confirm the stationary points.

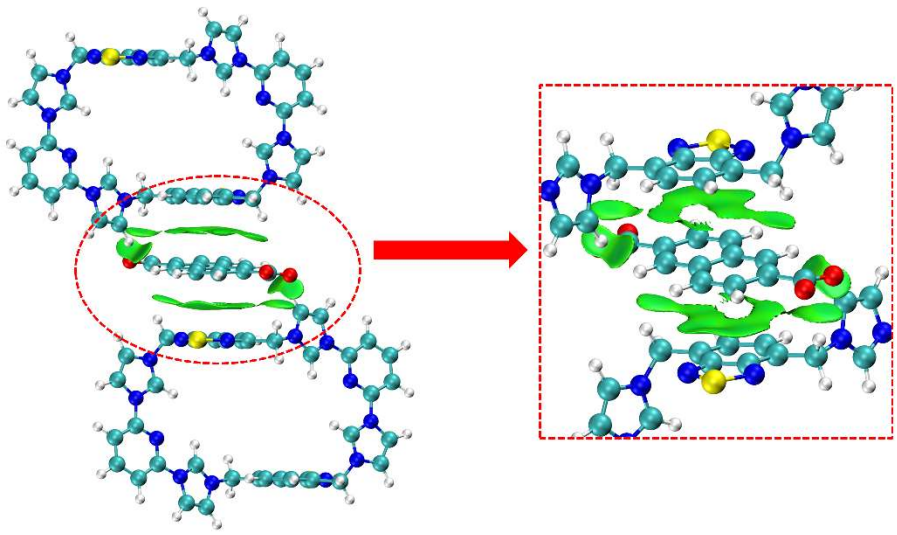

Fig. S49 The sign(λ_2)ρ colored isosurfaces of complex where guest $\mathbf{3}^{2-}$ was sandwiched between two $\mathbf{1}^{4+}$ molecules corresponding to IGMH analyses (δ_{ginter} = 0.004).

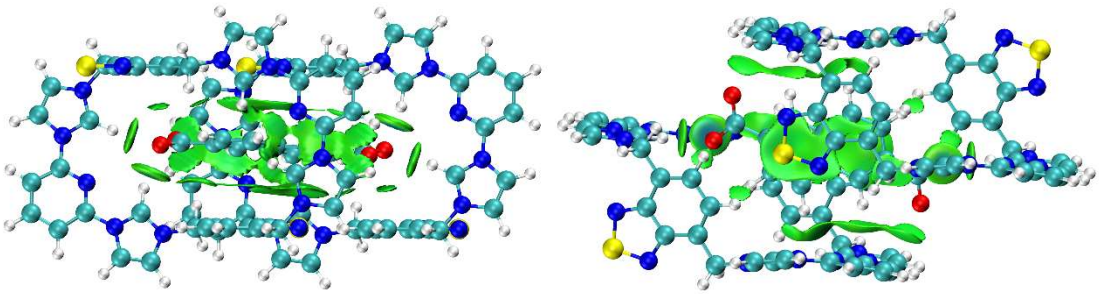

Fig. S50 The sign(λ_2)ρ colored isosurfaces of complex where guest $\mathbf{3}^{2-}$ was closed to the cavity of $\mathbf{1}^{4+}$ corresponding to IGMH analyses (δ_{ginter} = 0.004).

10. Characterization data and spectra

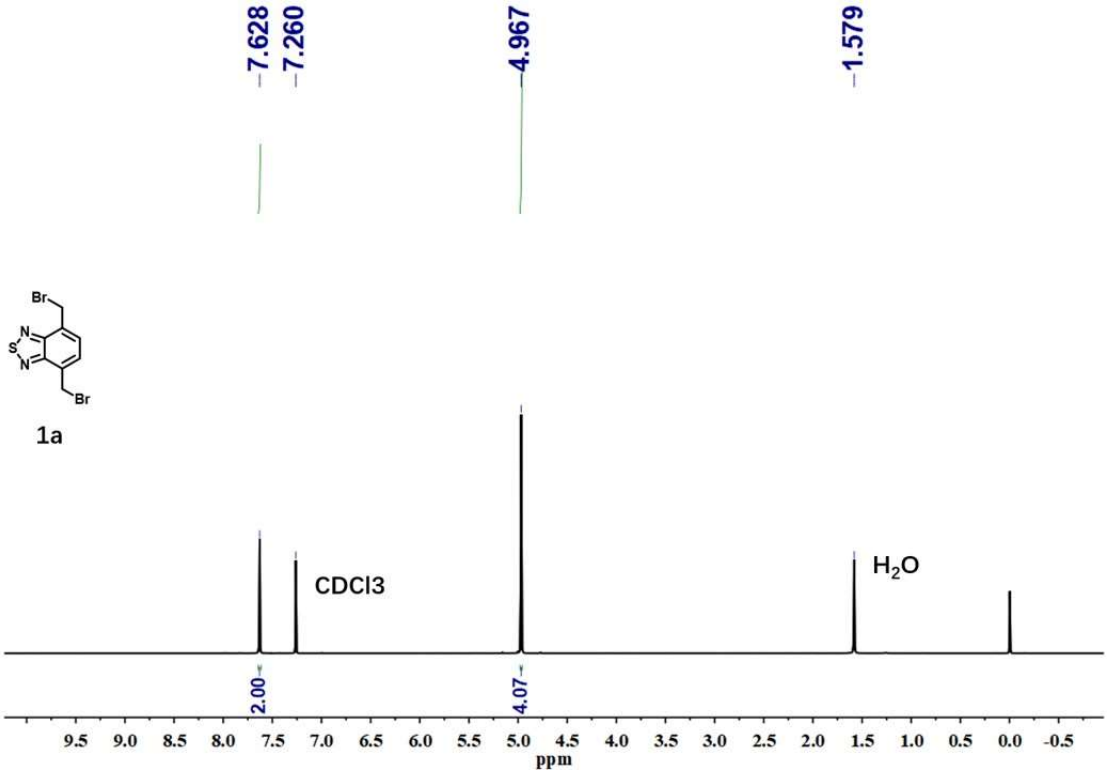

Fig. S51 ^{1}H NMR (400 MHz, $CDCl_3$, 298 K) spectrum of compound **1a**.

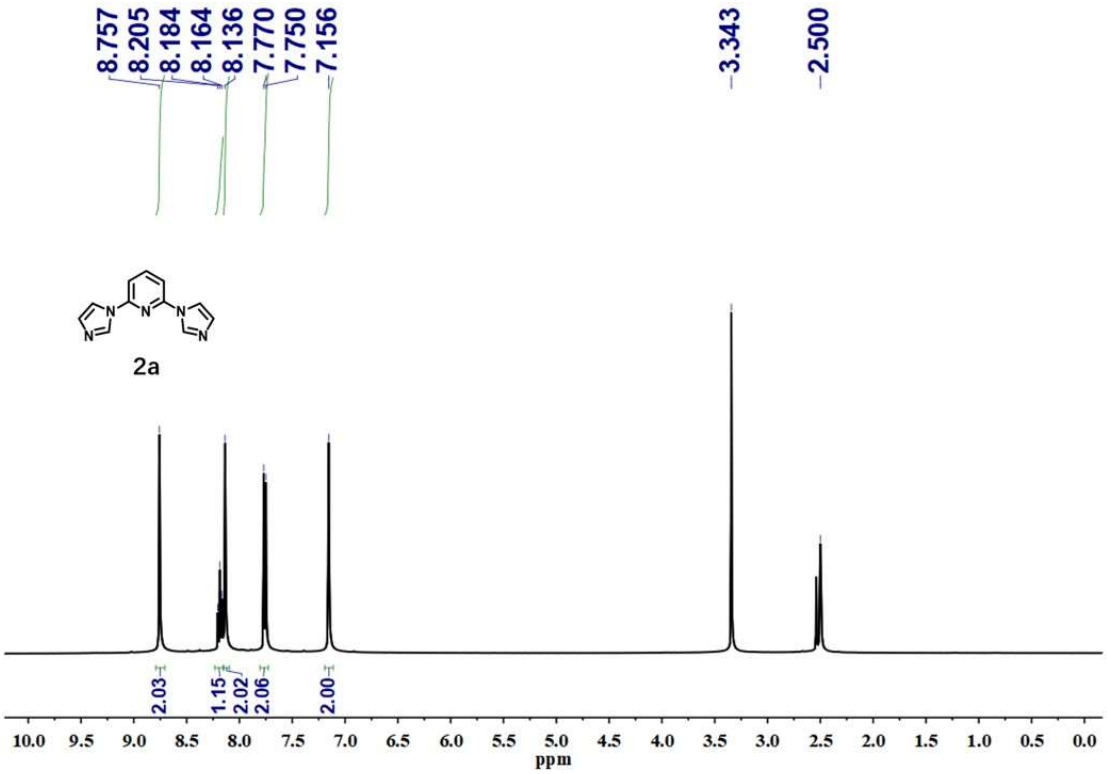

Fig. S52 ^{1}H NMR (400 MHz, $CDCl_3$, 298 K) spectrum of compound **2a**.

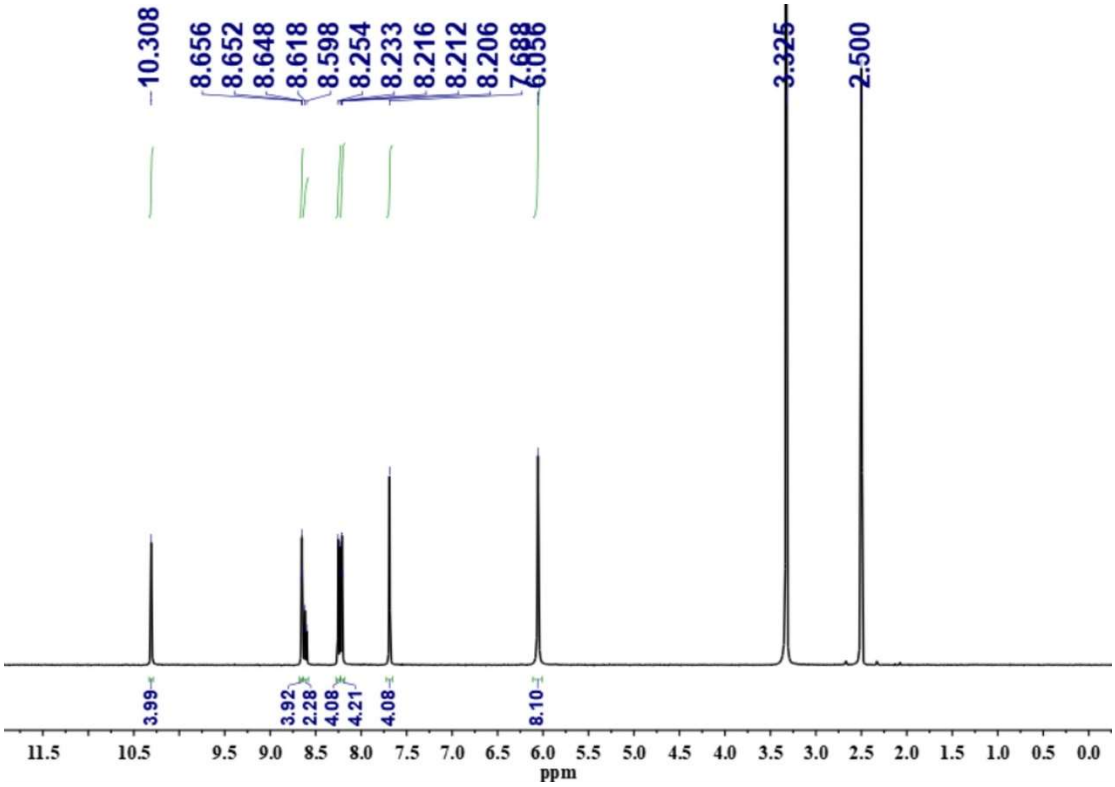

Fig. S53 ^{1}H NMR (400 MHz, DMSO-d_6, 298 K) spectrum of $\mathbf{1}^{4+}$•4PF_6^-.

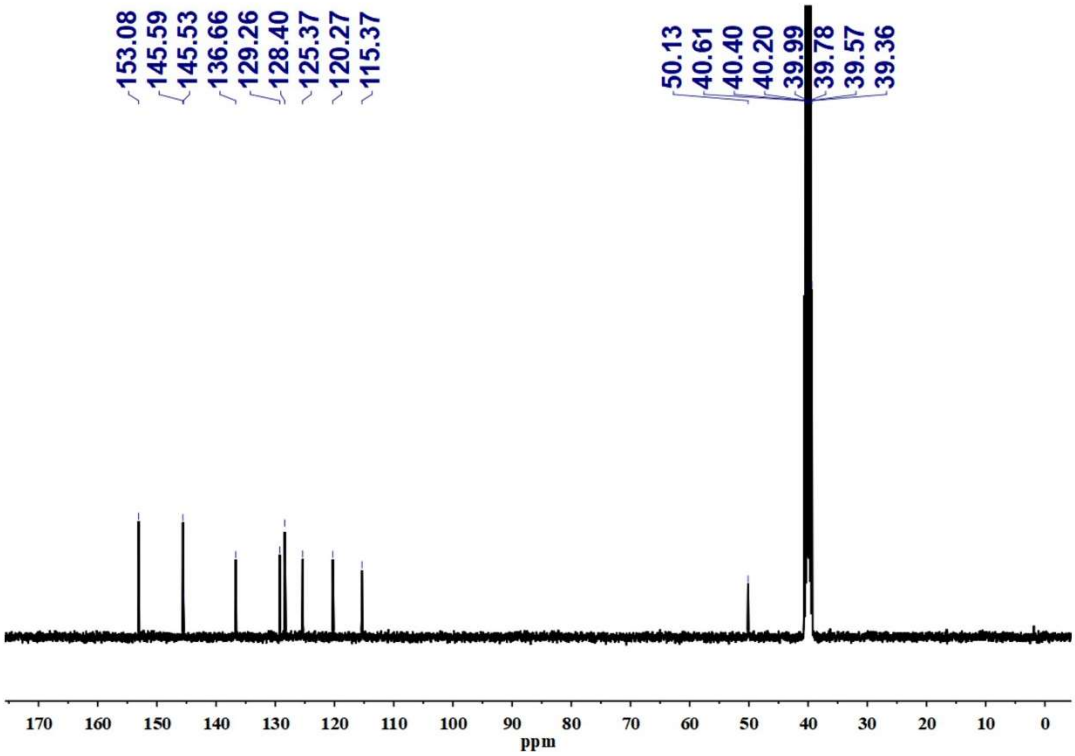

Fig. S54 ^{13C} NMR (100 MHz, DMSO-d_6, 298 K) spectrum of $\mathbf{1}^{4+}$•4PF_6^-.

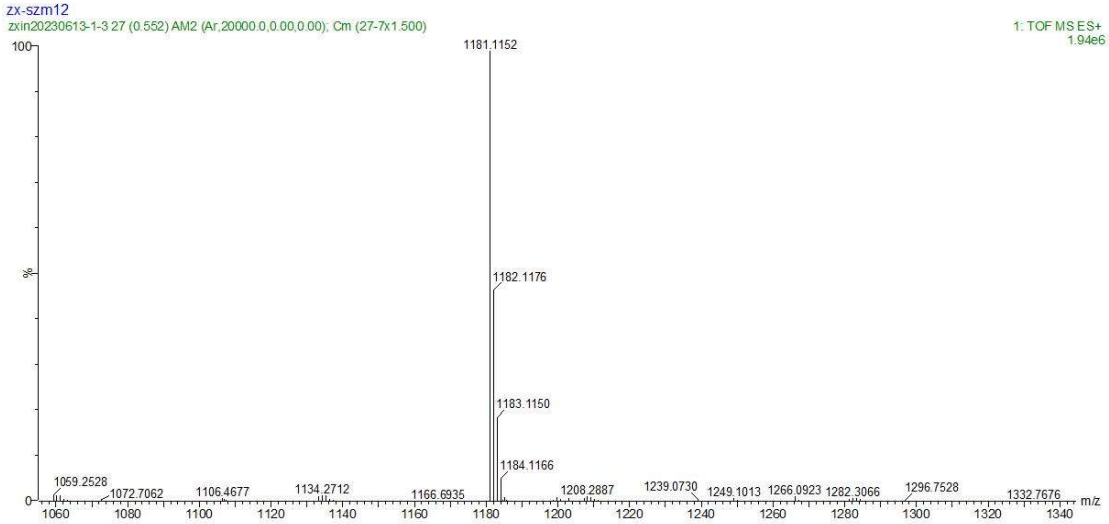

Fig. S55 HRMS spectrum of $\mathbf{1}^{4+}$•$4PF_6^-$.

11. Reference

[S1] Z. A. Page, Y. Liu, E. Puodziukynaite, T. P. Russell and T. Emrick, *Macromolecules,* 2016, **49**, 2526−2532.

[S2] V. Komanduri, D. J. Tate, R. Marcial-Hernandez, D. R. Kumar and M. L. Turner, *Macromolecules,* 2019, **52**, 7137−7144.

[S3] H. -Y. Gong, B. M. Rambo, E. Karnas, V. M. Lynch and J. L. Sessler, *Nat. Chem*., 2010, **2**, 406−409.

[S4] A. Caballero, E. Díez-Barra, F. A. Jalón, S. Merino and J. Tejeda, *J. Organomet. Chem*., 2001, **617–618**, 395-398.

[S5] K. Okuro, M. Furuune, M. Miura and M. Nomura, *J. Org. Chem*., 1993, **58**, 7606−7607.

[S6] S. Xie, P. Qin, M. Li, X. Zhang, Y. Jiang and D. M, *Tetrahedron Lett*., 2013, **54**, 3889−3891.

[S7] X. Wang, A. Guram, E. Bunel, G. Q. Cao, J. R. Allen and M. M. Faul, *J. Org. Chem*., 2008, **73**, 1643−1645.

[S8] X. Qian, J. Han and L. Wang, *Adv. Synth. Catal*., 2016, **358**, 940−946.

[S9] H. Brunne and P. Schmidt, *Eur. J. Org. Chem*., 2000, **2000**, 2119−2133.

[S10] C. Biagini, S. Albano, R. Caruso, L. Mandolini, J. A. Berrocal and S. Di Stefano, *Chem. Sci*., 2018, **9**, 181−188.

[S11] Job, P, *Ann. Chim. Paris*. 1928, **9**, 113−203.